22. Accelerated Life Test Models and Data Analysis

Today's consumers demand high quality and reliability in the products they buy. Accelerated life tests (ALT) are commonly used by manufacturers during product design to obtain reliability information on components and subsystems in a timely manner. The results obtained at high levels of the accelerating variables are then extrapolated to provide information about the product life under normal use conditions.

The introduction and Section 22.1 describe the background and motivations for using accelerated testing. Sections 22.2 and 22.3 discuss statistical models for describing lifetime distributions in ALT. Commonly used ALT models have two parts: (a) a statistical distribution at fixed levels of the accelerated variable(s); and (b) a functional relationship between distribution parameters and the accelerating variable(s). We describe relationships for accelerating variables, such as use rate, temperature, voltage, and voltage rate. We also discuss practical guidelines and potential problems in using ALT models. Section 22.4 describes and illustrates a strategy for analyzing ALT data. Both graphical and numerical methods are discussed for fitting an ALT model to data and for assessing its fit. These methods are thoroughly illustrated by fitting an ALT model with a single accelerating variable to data obtained from an actual ALT experiment. Extrapolation of the results at accelerated levels to normal use levels is also discussed. Section 22.5 presents statistical analysis of a wider variety of ALT data types that are encountered in practice. In particular, the examples involve ALTs with interval censoring and with two or more accelerating variables. Section 22.6 discusses practical considerations for interpreting statistical analysis of ALT data. This Section emphasizes the important role of careful planning of ALT to produce useful results. Section 22.7 discusses other kinds of accelerated tests often conducted in practice. Brief descriptions of each and specific applications in industry are also provided. Section 22.8 reviews some of the potential pitfalls the practitioner of accelerated testing may face. These are described within practical situations, and strategies for avoiding them are presented. Section 22.9 lists some computer software packages that are useful for analyzing ALT data.

Rapid developments in technology, consumer demand for highly reliable products, and competitive markets have placed pressure on manufacturers to deliver products with high quality and reliability. Similarly, there is strong pressure to shorten the concept-to-market cycle time, subject to the constraint of having a product with high reliability. Achieving these goals requires more attention to reliability early in the product design process and has lead to such programs as *design for reliability* and *design for six sigma.* As a result, there has been an increased need for upstream tests of product materials and components, often followed by subsequent testing of subsystems and even complete systems.

Customers may expect products to work properly for years or even decades. For instance, a refrigerator might be expected to work without failure for at least 10 years. Testing under normal operating conditions for reasonable lengths of time is unlikely to result in any failures and thus little information about product reliability. Hence, manufacturers perform accelerated tests (AT) on their products by exposing them to harsher conditions to generate failures and useful reliability information more quickly.

Depending on the nature of the product, life tests are accelerated by increasing product use rate or exposing the product to higher levels of accelerating variables such as temperature, pressure, and voltage. It is customary to fit a statistical model to the AT data and then extrapolate to use conditions to characterize the product's long-term performance. It is desirable that the statistical model for ATs be based on physical/chemical theory that can be used to justify the extrapolation. Operationally, however, detailed knowledge of theory relating the accelerating variables to life is not always available and the model is chosen on the basis of previous experience in similar situations.

Due to space constraints, we provide a limited discussion and description of the models and methods used in AT. For those actually involved in AT and for those who want more information, we highly recommend *Nelson* [22.1]. Other useful books with information that will complement this chapter include *Tobias* and *Trindade* [22.2] and *Meeker* and *Escobar* [22.3].

22.1 Accelerated Tests

22.1.1 Types of Accelerated Tests

During product design, manufacturers perform experiments to obtain timely information on material properties and component durability. Other experiments involving prototype systems and subsystems are used to help make product and process design decisions that will improve product robustness. Experiments are also run to support decision making in production process design. Tests during the production stage include certification of components, burn-in tests, and tests designed to monitor the production process over time. For further discussion of these issues, see *Meeker* and *Hamada* [22.4] and *Meeker* and *Escobar* [22.5]. Often these tests must be accelerated to obtain timely information.

ATs can be characterized by the nature of the response variable in the test (i. e., what can be measured or observed, relative to reliability):

- **Accelerated Life Tests ALT**
  The response in an ALT is related to the lifetime of the product. Often ALT data are right-censored because the test is stopped before all units fail. In other cases, the ALT response is interval-censored because failures are discovered at particular inspection times.
- **Accelerated Repeated Measures Degradation Tests ARMDT**

In an ARMDT, one measures degradation on a sample of units at different points in time. In general, each unit provides several degradation measurements. The degradation response could be actual chemical or physical degradation or performance degradation (e.g., drop in power output).

- **Accelerated Destructive Degradation Tests ADDT**
  An ADDT is similar to an ARMDT, except that the measurements are destructive, so one can obtain only one observation per test unit.

These different kinds of ATs can be closely related because they can involve the same underlying physical/chemical mechanisms for failure and models for acceleration. They are different, however, in that different kinds of statistical models and analyses are performed because of the differences in the kind of response.

This chapter focuses on analyses of data from ALTs. See *Meeker* and *Escobar* ([22.3], Chapts. 13 and 21) for further discussion of ARMDTs and see *Nelson* ([22.1], Chapt. 11) and *Meeker*, *Escobar*, *Kugler*, and *Kramer* [22.6] for models, methods, and examples pertaining to ADDTs.

22.1.2 Methods of Acceleration

There are different methods of accelerating tests to induce product failures more quickly. These methods vary depending on the nature of the product or material being tested.

- **Accelerate the Product Use Rate**
  This method is appropriate for products that are ordinarily not in continuous use. For example, the median life of a bearing for a certain washing machine agitator is 12 years, based on an assumed use rate of eight loads per week. If the machine is tested at 112 loads per week (16 per day), the median life is reduced to roughly 10 months.
- **Accelerate Product Aging**
  Changing environmental conditions (e.g., increasing humidity or temperature) can be used to increase the rate of chemical degradation of products such as insulating materials and adhesive bonds.
- **Accelerate by Increasing Product Stress**
  Increasing stress (e.g., voltage or pressure) on a specimen will generally cause it to fail sooner.

It is also possible to accelerate product failures by using combinations of these accelerating variables. For example, in fatigue testing one uses higher cycling rates and higher than usual levels of stress. In electro-chemical reactions, increasing voltage will also increase the rate of chemical change. Putting higher voltage stress on an insulating material may generate heat that will accelerate chemical change. In all types of acceleration, care should be taken to make sure that the underlying mechanisms and the resulting failure modes in an AT are the same as those that will affect the product in actual use.

22.1.3 Choosing an Accelerated Life Test Model

The task of finding an ALT model can be divided into two steps:

1. Choose an appropriate statistical distribution to describe lifetime at fixed levels of the accelerating variable(s). Typically the same distribution is used at all levels of stress, as would be suggested by the commonly used scale-accelerated failure-time, SAFT, model. Probability plots (i. e., plotting a nonparametric estimate on special distribution-specific probability scales) are used to help identify an appropriate distribution.
2. Choose a model to describe the relationship between the lifetime distributions and the accelerating variables. It is best if the selected model is based on physical or chemical theory, empirical considerations, or both.

These two steps are discussed in detail in Sects. 22.2 and 22.3, respectively.

As will be discussed in subsequent sections, the combination of probability plotting and maximum likelihood provides the basic statistical tools for analyzing most ALT data. Probability plots provide a convenient, intuitive method to display ALT data and assess agreement with proposed models for the data. These methods are described in detail in *Nelson* ([22.1], Chapt. 3) and *Meeker* and *Escobar* ([22.3], Chapts. 6 and 19). Maximum likelihood (ML) is the most common method of fitting an ALT model to data because it allows for censored data and because ML estimates have desirable statistical properties. The ML estimates of model parameters are those parameter values that maximize the probability of the observed data for the proposed model. The theory of ML methods has been thoroughly explored in the literature. *Nelson* ([22.1], Chapt. 5) and *Meeker* and *Escobar* ([22.3], Chapts. 8 and 19) discuss ML methods relevant to ALT data analysis. Both probability plotting and maximum likelihood methods are now widely available in commercial statistical software, as described in Sect. 22.9.

22.2 Life Distributions

In this chapter, the symbol T will denote lifetime for devices, components, systems, etc. Then, it will be assumed that T is a positive continuous random variable. The cumulative distribution function CDF for T is the probability of failure by time t (or the fraction failing by time t) and one writes $F(t) = \Pr(T \le t)$. The probability density function PDF $f(t)$ is the derivative of the CDF. That is, $f(t) = \mathrm{d}F(t)/\mathrm{d}t$. Selecting a probability distribution for lifetime is equivalent to specifying either $F(t)$ or $f(t)$.

This section describes log-location-scale probability distributions. Important members of this family include the popular Weibull and lognormal distributions. Other members of the family are described in Chapt. 4 of *Meeker* and *Escobar* [22.3]. Distributions that are other than log-location-scale (which could also be used in ALT modeling) are described in Chapt. 5 of *Meeker* and *Escobar* [22.3].

A random variable Y has a location-scale distribution if its CDF can be written as

$$F(y;\mu,\sigma) = \Pr(Y \le y) = \Phi\left(\frac{y-\mu}{\sigma}\right) ,$$

where μ is a location parameter, σ is a scale parameter, and Φ does not depend on any unknown parameters. In many reliability applications, it is assumed that $\log(T)$ has a location-scale distribution. Then T is said to have a log-location-scale distribution.

22.2.1 The Lognormal Distribution

Lifetime T has a lognormal distribution if its CDF and PDF are

$$F(t;\mu,\sigma) = \Phi_{\mathrm{nor}}\left(\frac{\log(t)-\mu}{\sigma}\right) ,$$

$$f(t;\mu,\sigma) = \frac{1}{\sigma t}\phi_{\mathrm{nor}}\left(\frac{\log(t)-\mu}{\sigma}\right) , \quad t > 0 ,$$

where Φ_{nor} and ϕ_{nor} are the standard normal (Gaussian) CDF and PDF, respectively. In particular,

$$\phi_{\mathrm{nor}}(z) = \frac{1}{\sqrt{2\pi}}\exp\left(-\frac{z^2}{2}\right) .$$

The parameters (μ,σ) are the mean and the standard deviation of $\log(T)$, respectively. Then $[\exp(\mu),\sigma]$ are, respectively, the scale and shape parameters of T. The lognormal p quantile is $t_p = \exp[\mu + \Phi^{-1}_{\mathrm{nor}}(p)\,\sigma]$. Note that $\exp(\mu)$ corresponds to the median lifetime. That is, $t_{0.50} = \exp(\mu)$.

22.2.2 The Weibull Distribution

Lifetime T has a Weibull distribution if its CDF and PDF are

$$\begin{aligned} F(t;\mu,\sigma) &= \Phi_{\mathrm{sev}}\left(\frac{\log(t)-\mu}{\sigma}\right) \\ &= 1-\exp\left[-\left(\frac{t}{\eta}\right)^{\beta}\right] \\ f(t;\mu,\sigma) &= \frac{1}{\sigma t}\phi_{\mathrm{sev}}\left(\frac{\log(t)-\mu}{\sigma}\right) \\ &= \frac{\beta}{\eta}\left(\frac{t}{\eta}\right)^{\beta-1}\exp\left[-\left(\frac{t}{\eta}\right)^{\beta}\right], \quad t > 0, \end{aligned}$$

where Φ_{sev} and ϕ_{sev} are the standard smallest extreme value SEV CDF and PDF defined by

$$\Phi_{\mathrm{sev}}(z) = 1-\exp[-\exp(z)]$$
$$\text{and} \quad \phi_{\mathrm{sev}}(z) = \exp[z-\exp(z)] ,$$

$\sigma > 0$, and $-\infty < \mu < \infty$. Here (μ,σ) are the location and scale parameters for the distribution of $\log(T)$. The expressions for the CDF and PDF above also use $\eta = \exp(\mu)$ and $\beta = 1/\sigma$, the traditional Weibull scale and shape parameters, respectively. The Weibull p quantile is $t_p = \exp\{\mu + \log[-\log(1-p)]\,\sigma\} = \eta[-\log(1-p)]^{\beta}$. Note that η is approximately the 0.63 quantile of the Weibull distribution.

The parameterization in terms of (μ,σ) is particularly convenient for lifetime regression models and is used extensively in this chapter. The (η,β) parameterization is commonly used in the engineering and statistical literature.

22.3 Acceleration Models

fitting a model to data obtained at high levels of the accelerating variables and extrapolating the results to use conditions levels. Ideally, this model should be derived from physical or chemical theory and verified empirically to justify the extrapolation. If a physical understanding of the failure mechanism is lacking, an

empirical model might be justified for extrapolation if it is based on extensive experience with how failure mechanisms relate to accelerating variables.

This section discusses basic ideas of acceleration models and some physical considerations that lead to these models. For more information on these models, see *Nelson* ([22.1], Chapt. 2) and *Meeker* and *Escobar* ([22.3], Chapt. 18).

22.3.1 Scale-Accelerated Lifetime Model

A simple, commonly used model used to characterize the effect that explanatory variables $\boldsymbol{x} = (x_1, \ldots, x_k)'$ have on lifetime T is the scale-accelerated failure-time (SAFT) model. Some of these explanatory variables are accelerating, but others may just be of interest (e.g., for product design optimization decisions). If $\boldsymbol{x}_U$ denotes the ordinary use conditions, under a SAFT model, lifetime at $\boldsymbol{x}$, $T(\boldsymbol{x})$, is scaled by a deterministic factor that might depend on $\boldsymbol{x}$ and unknown fixed parameters. More specifically, $T(\boldsymbol{x}) = T(\boldsymbol{x}_U)/\mathcal{AF}(\boldsymbol{x})$ where the *acceleration factor* $\mathcal{AF}(\boldsymbol{x})$ is a positive function of $\boldsymbol{x}$ satisfying $\mathcal{AF}(\boldsymbol{x}_U) = 1$. Lifetime is accelerated (decelerated) when $\mathcal{AF}(\boldsymbol{x}) > 1$ [$\mathcal{AF}(\boldsymbol{x}) < 1$]. Some special cases of these important SAFT models are discussed in the following sections.

Observe that under a SAFT model, the probability that failure under conditions $\boldsymbol{x}$ occurs at or before time t can be written as $\Pr[T(\boldsymbol{x}) \le t] = \Pr[T(\boldsymbol{x}_U) \le \mathcal{AF}(\boldsymbol{x}) \times t]$. As described in Sect. 22.2, it is common practice to assume that the lifetime $T(\boldsymbol{x})$ has a log-location-scale distribution such as a lognormal or Weibull distribution in which μ is a function of the accelerating variable(s) and σ is constant (i. e., does not depend on $\boldsymbol{x}$). In this case,

$$F(t; \boldsymbol{x}_U) = \Pr[T(\boldsymbol{x}_U) \le t] = \Phi\left(\frac{\log(t) - \mu_U}{\sigma}\right), \tag{22.1}$$

where Φ denotes a standard cumulative distribution function (e.g., standard normal or standard smallest extreme value) and μ_U is the location parameter for the distribution of $\log[T(\boldsymbol{x}_U)]$. Thus,

$$F(t; \boldsymbol{x}) = \Pr[T(\boldsymbol{x}) \le t] = \Phi\left(\frac{\log(t) - \{\mu_U - \log[\mathcal{AF}(\boldsymbol{x})]\}}{\sigma}\right). \tag{22.2}$$

Note that $T(\boldsymbol{x})$ also has a log-location-scale distribution with location parameter $\mu = \mu_U - \log[\mathcal{AF}(\boldsymbol{x})]$ and a scale parameter σ that does not depend on $\boldsymbol{x}$.

22.3.2 Accelerating Product Use Rate

Increasing the use rate can be an effective method of acceleration for some products. In simple situations the cycles-to-failure distribution does not depend on the cycling rate. In such situations *reciprocity holds*. Then the underlying model for lifetime is SAFT where $\mathcal{AF}(\text{UseRate}) = \text{UseRate}/\text{UseRate}_U$ is the factor by which the test is accelerated.

Use-rate acceleration may be appropriate for products such as electrical relays and switches, paper copiers, and printers, and home appliances such as toasters and washing machines. The manner in which the use rate is increased may depend on the product. For example, *Nelson* ([22.1], page 16) states that failure of rolling bearings can be accelerated by running them at three or more times the normal speed. *Johnston* et al. [22.7] demonstrated that the cycles-to-failure of electrical insulation was shortened, approximately, by a factor of $\mathcal{AF}(412) = 412/60 \approx 6.87$ when the applied AC voltage in endurance tests was increased from 60 Hz to 412 Hz.

ALTs with increased use rate attempt to simulate actual use. Thus other environmental factors should be controlled to mimic actual use environments. If the cycling rate is too high, it can cause *reciprocity breakdown*. For example it may be necessary to have test units (such as a toaster) cool down between cycles of operation. *Dowling* ([22.8], page 706) describes how increased cycle rate may affect the crack growth rate in per-cycle fatigue testing.

Reciprocity breakdown is known to occur, for example, for certain components in copying machines where components tend to last longer (in terms of cycles) when printing is done at higher rates. In such cases, the empirical power-rule relationship $\mathcal{AF}(\text{UseRate}) = (\text{UseRate}/\text{UseRate}_U)^p$ is often used, where p can be estimated by testing at two or more use rates.

22.3.3 Models for Temperature Acceleration

This section describes common models that are used to describe the relationship between lifetime and temperature.

The Arrhenius Relationship for Temperature Acceleration

The Arrhenius equation is widely used to relate the rate of a chemical reaction $\mathcal{R}$ to temperature temp. This relationship can be written as

$$\mathcal{R}(\text{temp}) = \gamma_0 \exp\left(\frac{-E_a}{k_B \times \text{temp K}}\right) = \gamma_0 \exp\left(\frac{-E_a \times 11605}{\text{temp K}}\right), \quad (22.3)$$

where γ_0 and the activation energy E_a are constants that depend on material properties and test methods, $k_B = 8.6171 \times 10^{-5} = 1/11605$ is Boltzmann's constant in units of electron volts per °C, and temp K = temp °C + 273.15 is the temperature kelvin. The Arrhenius lifetime relationship is based on the view that failure occurs after there has been a critical amount of chemical reaction. Then when $\mathcal{R}$(temp) is larger, the failure will occur sooner (e.g., *Klinger* [22.9]). Empirical observations have suggested that the Arrhenius equation provides an adequate description of the relationship between product life and temperature in a variety of applications such as integrated circuits (several different kinds of failure modes), light-emitting diodes (LEDs), adhesive bonds, lubricants, incandescent bulb filaments, insulating tapes, and dielectric materials. It should be noted, however, that the nature of the failure mechanism may limit the range of temperature over which the Arrhenius relationship is adequate.

Let temp_U be the temperature at use conditions. Then the Arrhenius acceleration factor is

$$\mathcal{AF}(\text{temp}, \text{temp}_U, E_a) = \frac{\mathcal{R}(\text{temp})}{\mathcal{R}(\text{temp}_U)} = \exp\left[E_a\left(\frac{11605}{\text{temp}_U \text{ K}} - \frac{11605}{\text{temp K}}\right)\right].$$

For simplicity, the time-acceleration factor is sometimes written as $\mathcal{AF}$(temp) instead of $\mathcal{AF}(\text{temp}, \text{temp}_U, E_a)$.

Let $\text{temp}_{Low} < \text{temp}_{High}$ be two temperature levels and define the temperature differential factor TDF

$$\text{TDF} = \left(\frac{11605}{\text{temp}_{Low} \text{ K}} - \frac{11605}{\text{temp}_{High} \text{ K}}\right). \quad (22.4)$$

Then, one can write

$$\mathcal{AF}(\text{temp}_{High}, \text{temp}_{Low}, E_a) = \exp(E_a \times \text{TDF}). \quad (22.5)$$

Example 22.1: Adhesive-Bonded Power Element. *Meeker* and *Hahn* [22.10] describe an adhesive-bonded power element that was designed for use at temp = 50 °C and a life test of this element is to be conducted at temp = 120 °C. Suppose that experience with this product suggested that $E_a = 0.5$. Using (22.4) and (22.5) gives TDF = 6.39 and then $\mathcal{AF}(120) \approx 24.41$ gives the acceleration factor for the chemical reaction when testing the power element at 120 °C.

Note that the Arrhenius relationship (and the assumption that the failure is directly related to the amount of material reacting) implies that the acceleration model is a SAFT model. If $T(\text{temp}_U)$ has a log-location-scale distribution with parameters μ_U and σ, then it follows from (22.2) that T(temp) also has a log-location-scale distribution with parameters $\mu = \mu_U - \beta_1 x$ and σ, where $\beta_1 = E_a$, $x =$ TDF, and the TDF is computed for the temperatures $\text{temp}_U <$ temp.

Nonlinear Degradation Path Models for Reaction-Rate Acceleration

As discussed earlier, when failure is caused directly by degradation, one can relate the distribution of degradation to the distribution of failure. Suppose that failure occurs when degradation reaches a certain critical level $\mathcal{D}_f$. This section discusses the situation in which degradation follows a nonlinear path (e.g., the degradation path will reach an asymptote because of a limited amount of material that is available to go into the reaction) over time. The linear path case is discussed in the next section.

The amount of degradation at time t and temperature temp is given by

$$\mathcal{D}(t; \text{temp}) = \mathcal{D}_\infty \times \left\{1 - \exp\left[-\mathcal{R}_U \times \mathcal{AF}(\text{temp}) \times t\right]\right\}, \quad (22.6)$$

where $\mathcal{R}_U$ is the rate of reaction rate at the use temperature temp_U. Note that $\mathcal{R}_U \times \mathcal{AF}$(temp) is the rate reaction at temp and $\mathcal{AF}(\text{temp}) > 1$ when $\text{temp} > \text{temp}_U$. Figure 22.1 shows the decrease in strength of adhesive bonds, as a function of time for different temperatures. In this application, $\mathcal{D}_\infty < 0$ so that, for fixed temp, $\mathcal{D}(t; \text{temp})$ is a decreasing function of t and failure occurs when $\mathcal{D}(t; \text{temp})$ falls below $\mathcal{D}_f$, say 50 N. In other applications, $\mathcal{D}_\infty > 0$, then $\mathcal{D}(t; \text{temp})$ is increasing and failure occurs once $\mathcal{D}(t; \text{temp})$ exceeds $\mathcal{D}_f$. For both cases, the lifetime T(temp) at any level temp is given by $T(\text{temp}) = T(\text{temp}_U)/\mathcal{AF}(\text{temp})$ where $T(\text{temp}_U) = -(1/\mathcal{R}_U)\log(1 - \mathcal{D}_f/\mathcal{D}_\infty)$. Note that this has the form of a SAFT model. Sufficient

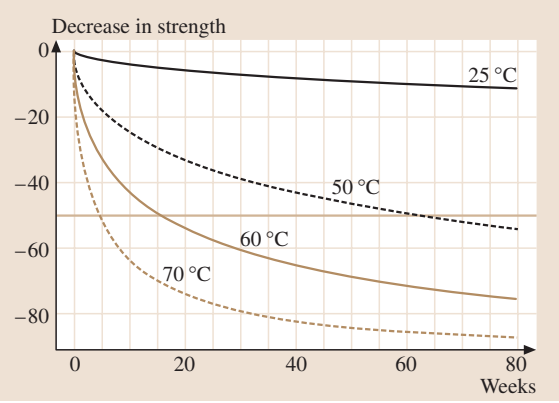

Fig. 22.1 Nonlinear decreasing degradation path at different temperatures for a SAFT model

conditions for a degradation model to be SAFT are given by *LuValle*, *Welsher* and *Svoboda* [22.11] and *Klinger* [22.9]. Under a SAFT model and a log-location-scale distribution with parameters μ and σ for $T(\text{temp}_\text{U})$, $T(\text{temp})$ at any temp also has a log-location-scale distribution with the same σ and

$$\mu = \mu_\text{U} - \log\left[\mathcal{AF}(\text{temp})\right] = \beta_0 + \beta_1 x,$$

where $x = 11605/(\text{tempK})$, $x_\text{U} = 11605/(\text{temp}_\text{U}\text{K})$, $\beta_1 = E_\text{a}$, $\beta_0 = \mu_\text{U} - \beta_1 x_\text{U}$, and μ_U is the location parameter of the distribution of $\log(T)$ at use conditions.

Linear Degradation Path Models for Reaction-Rate Acceleration

There are situations in which a linear model can be used to approximate degradation over time. For example, when $\mathcal{R}_\text{U} \times \mathcal{AF}(\text{temp}) \times t$ in (22.6) is small enough so that $\mathcal{D}(t)$ is small compared to $\mathcal{D}_\infty$, then

$$\begin{aligned}\mathcal{D}(t;\text{temp}) &= \mathcal{D}_\infty \times \left\{1 - \exp\left[-\mathcal{R}_\text{U} \times \mathcal{AF}(\text{temp}) \times t\right]\right\} \\ &\approx \mathcal{D}_\infty \times \mathcal{R}_\text{U} \times \mathcal{AF}(\text{temp}) \times t = \mathcal{R}_\text{U}^+ \times \mathcal{AF}(\text{temp}) \times t\,,\end{aligned}$$

where $\mathcal{R}_\text{U}^+ = \mathcal{D}_\infty \times \mathcal{R}_\text{U}$. There are also practical situations (e.g., wear of automobile tires) for which a linear path adequately approximates degradation over time. In this case, $\mathcal{D}(t;\text{temp}) = \mathcal{R}_\text{U}^+ \times \mathcal{AF}(\text{temp}) \times t$ where it is assumed that $\mathcal{D}(0;\text{temp}) = 0$ and that $\mathcal{R}_\text{U}^+ \times \mathcal{AF}(\text{temp})$ is the degradation rate at condition temp.

Again, failure occurs when $\mathcal{D}(t;\text{temp})$ reaches a critical level $\mathcal{D}_\text{f}$. The equation $\mathcal{D}(t;\text{temp}) = \mathcal{D}_\text{f}$ yields the lifetime at temp, $T(\text{temp}) = T(\text{temp}_\text{U})/\mathcal{AF}(\text{temp})$ which, again, is in SAFT form. Thus, if $T(\text{temp})$ has a log-location-scale distribution, $\mu = \beta_0 + \beta_1 x$ and σ does not depend on x (where x has the same definition given in Sect. 22.3.3).

22.3.4 Models for Voltage and Voltage–Stress Acceleration

Voltage or voltage stress can also be used to accelerate degradation and hasten product failures. Voltage measures the amount of force needed to move an electric charge between two points. Such a flow of charges produces an electrical current. Voltage stress measures voltage per unit of thickness of a dielectric. For dielectric components (e.g., capacitors and insulators), chemical degradation reduces the dielectric strength over time. Also, stronger electric fields can accelerate the growth of discontinuities, electrochemical reactions, or electromechanical changes that cause failure.

Example 22.2: Accelerated Life Test of Insulation for Generator Armature Bars. *Doganaksoy* et al. [22.12] discuss an ALT for a new mica-based insulation design for generator armature bars GAB. Degradation of an organic binder in the insulation causes a decrease in voltage strength and this was the primary cause of failure in the insulation. The insulation was designed for use at a voltage stress of 120 V/mm. Voltage-endurance tests were conducted on 15 electrodes at each of five accelerated voltage levels between 170 V/mm and 220 V/mm (i. e., a total of 75 electrodes). Each test was run for 6480 h at which point 39 of the electrodes had not yet failed. Table 22.1 gives the data from these tests. The insulation engineers were interested in the 0.01 and 0.05 quantiles of lifetime at the use condition of

Table 22.1 GAB insulation data

Voltage stress (V/mm)	Lifetime (10^3 h)
170	15 censored[a]
190	3.248, 4.052, 5.304, 12 censored[a]
200	1.759, 3.645, 3.706, 3.726, 3.990, 5.153, 6.368, 8 censored[a]
210	1.401, 2.829, 2.941, 2.991, 3.311, 3.364, 3.474, 4.902, 5.639, 6.021, 6.456, 4 censored[a]
220	0.401, 1.297, 1.342, 1.999, 2.075, 2.196, 2.885, 3.019, 3.550, 3.566, 3.610, 3.659, 3.687, 4.152, 5.572

[a] Units were censored at 6.480 10^3 h

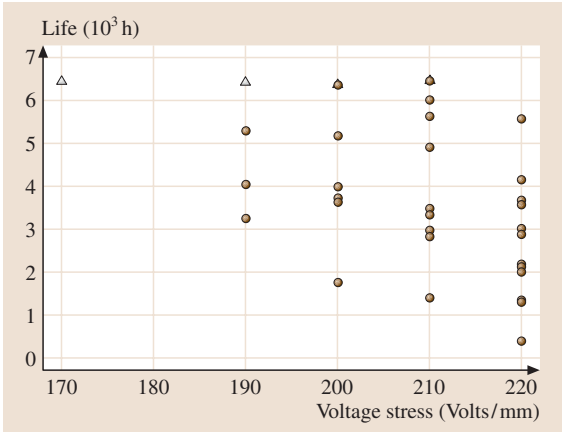

Fig. 22.2 GAB insulation data. Scatter plot of life versus voltage. Censored observations are indicated by Δ

120 V/mm. Figure 22.2 plots the insulation lifetimes against voltage stress.

Inverse Power Relationship

The inverse power relationship is frequently used to describe the effect that stresses like voltage and pressure have on lifetime. Voltage is used in the following discussion. When the thickness of a dielectric material or insulation is constant, voltage is proportional to voltage stress. Let volt denote voltage and let volt_U be the voltage at use conditions. The lifetime at stress level volt is given by

$$T(\text{volt}) = \frac{T(\text{volt}_\text{U})}{\mathcal{AF}(\text{volt})} = \left(\frac{\text{volt}}{\text{volt}_\text{U}}\right)^{\beta_1} T\,(\text{volt}_\text{U})\ ,$$

where β_1, in general, is negative. The model has SAFT form with acceleration factor

$$\mathcal{AF}(\text{volt}) = \mathcal{AF}(\text{volt}, \text{volt}_\text{U}, \beta_1) = \frac{T(\text{volt}_\text{U})}{T(\text{volt})} = \left(\frac{\text{volt}}{\text{volt}_\text{U}}\right)^{-\beta_1}\ . \qquad (22.7)$$

If $T(\text{volt}_\text{U})$ has a log-location-scale distribution with parameters μ_U and σ, then $T(\text{volt})$ also has a log-location-scale distribution with $\mu = \beta_0 + \beta_1 x$, where $x_\text{U} = \log(\text{volt}_\text{U})$, $x = \log(\text{volt})$, $\beta_0 = \mu_\text{U} - \beta_1 x_\text{U}$, and σ does not depend on x.

Example 22.3: Time Acceleration for GAB Insulation. For the GAB insulation data in Example 22.2, an estimate for β_1 is $\hat{\beta}_1 = -9$ (methods for computing such estimates are described and illustrated in Sect. 22.4). Recall that the design voltage stress is $\text{volt}_\text{U} = 120\,\text{V/mm}$ and consider testing at volt = 210 V/mm. Thus, using $\beta_1 = \hat{\beta}_1$, $\mathcal{AF}(210) = (210/120)^9 \approx 154$. Thus by increasing voltage stress from 120 to 210 V/mm, one estimates that lifetime is shortened by a factor of $1/\mathcal{AF}(210) \approx 1/154 = 0.0065$. Figure 22.3 plots $\mathcal{AF}$ versus volt for $\beta_1 = -7, -9, -11$. Using direct computations or from the plot, one obtains $\mathcal{AF}(210) \approx 50$ for $\beta_1 = -7$ and $\mathcal{AF}(210) \approx 471$ for $\beta_1 = -11$.

Motivation for the Inverse Power Relationship

The following description of a failure process that relates lifetime to pressure-like stresses, leading to the inverse power relationship, comes from *Meeker* and *Escobar* ([22.3], Sect. 18.4.3). Insulation units or specimens will have a characteristic dielectric strength $\mathcal{D}$. This property varies from unit to unit and degrades over time. When $\mathcal{D}$ degrades to the level of the applied voltage stress volt, a failure-causing event (e.g., short circuit or a flash-over) is triggered. Suppose one can express the dielectric strength at time t by $\mathcal{D}(t) = \delta_0 \times t^{1/\beta_1}$. Letting $\mathcal{D}(t) = \text{volt}$ and solving for t, $T(\text{volt}) = (\text{volt}/\delta_0)^{\beta_1}$. The acceleration factor for comparing lifetimes at volt and volt_U is

$$\mathcal{AF}(\text{volt}) = \mathcal{AF}(\text{volt}, \text{volt}_\text{U}, \beta_1) = \frac{T(\text{volt}_\text{U})}{T(\text{volt})} = \left(\frac{\text{volt}}{\text{volt}_\text{U}}\right)^{-\beta_1}\ ,$$

which agrees with (22.7).

The inverse power relationship can be used to describe cases for which the accelerating voltage increases the degradation rate. For example, suppose that degra-

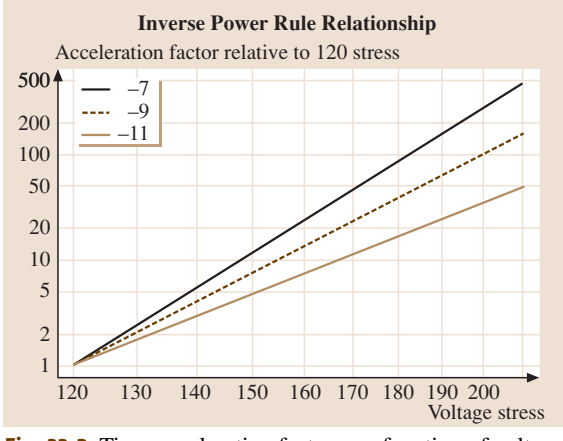

Fig. 22.3 Time-acceleration factor as a function of voltage stress and exponent $-\beta_1 = -7, -9, -11$

dation is more appropriately described by

$$\mathcal{D}(t) = \delta_0 \left[\mathcal{R}(\text{volt}) \times t\right]^{1/\gamma_1} ,$$

where $\mathcal{R}(\text{volt}) = \gamma_0 \exp\left[\gamma_2 \log(\text{volt})\right]$. Again, if failure occurs when $\mathcal{D}_\text{f} = \text{volt}$, then lifetime is

$$T(\text{volt}) = \frac{1}{\mathcal{R}(\text{volt})} \left(\frac{\text{volt}}{\delta_0}\right)^{\gamma_1} .$$

Then the acceleration factor is

$$\mathcal{AF}(\text{volt}) = \frac{T(\text{volt}_\text{U})}{T(\text{volt})} = \left(\frac{\text{volt}}{\text{volt}_\text{U}}\right)^{\gamma_2 - \gamma_1}$$

which is an inverse power relationship with $\beta_1 = \gamma_1 - \gamma_2$.

This discussion can be extended to other materials and products such as filaments of light bulbs, capacitors, roller bearings, and ball bearings. The inverse power relationship has also been used with other accelerating factors such as loading stress, cycling rate, humidity, and pressure.

22.3.5 Models for Two-or-More-Variable Acceleration

Some ALTs use two or more accelerating variables that affect the degradation process. In comparison with single-variable ALTs, in some situations, the degradation rate can be increased more effectively when two or more variables are used to accelerate the test. Many ALTs use temperature in combination with another environmental condition such as pressure, voltage, and humidity. The rest of this section describes models for these ALTs.

Extending the Arrhenius Relationship

Recall the Arrhenius equation (22.3), which gives the rate of a chemical reaction as a function of temperature. Suppose that X represents a non-thermal accelerating variable. A model for reaction rate in this situation is

$$\mathcal{R}(\text{temp}, X) = \gamma_0 \times \exp\left(\frac{-\gamma_1}{k_\text{B} \times \text{temp K}}\right) \times \exp\left(\gamma_2 X + \frac{\gamma_3 X}{k_\text{B} \times \text{temp K}}\right) , \quad (22.8)$$

where the parameters $\gamma_1 = E_\text{a}$ (the effective activation energy), γ_0, γ_2, and γ_3 are specific properties of the failure-causing chemical reaction. In (22.8), the ratio $\gamma_3 X/(k_\text{B} \times \text{temp K})$ represents possible interaction between the two accelerating variables. This model could be further extended by adding appropriate factors for other explanatory variables to the right-hand side of (22.8).

Using a SAFT formulation, one can equivalently express the extended Arrhenius relationship (22.8) in terms of the acceleration factor given by

$$\mathcal{AF}(\text{temp}, X) = \frac{\mathcal{R}(\text{temp}, X)}{\mathcal{R}(\text{temp}_\text{U}, X_\text{U})} . \quad (22.9)$$

When $T(\text{temp}_\text{U}, X_\text{U})$ has a log-location-scale distribution, (22.1), (22.8) and (22.9) imply that $T(\text{temp}, X)$ also has a log-location-scale distribution with

$$\begin{aligned}\mu &= \mu_\text{U} - \log[\mathcal{AF}(\text{temp}, X)] \\ &= \beta_0 + \beta_1 x_1 + \beta_2 x_2 + \beta_3 x_1 x_2 ,\end{aligned} \quad (22.10)$$

where $\beta_1 = E_\text{a}$, $\beta_2 = -\gamma_2$, $\beta_3 = -\gamma_3$, $x_1 = 11605/(\text{temp K})$, $x_2 = X$, $\beta_0 = \mu_\text{U} - \beta_1 x_{1\text{U}} - \beta_2 x_{2\text{U}} - \beta_3 x_{1\text{U}} x_{2\text{U}}$, and σ does not depend on the explanatory variables (temp, X).

Temperature–Voltage Acceleration Models

There has been a variety of approaches that have been used to model the combination of temperature and voltage acceleration. For instance, *Meeker* and *Escobar* ([22.3], Sect. 17.7) analyzed data from a study relating voltage and temperature to the failure of glass capacitors. They modeled the location parameter of log lifetime as a simple linear function of temp °C and volt. The extended Arrhenius relationship in Sect. 22.3.5 can also be used with $X = \log(\text{volt})$, as in *Boyko* and *Gerlach* [22.13]. *Klinger* [22.14] modeled the *Boyko* and *Gerlach* [22.13] data by including second-order terms for both accelerating variables.

To derive the time-acceleration factor for the extended Arrhenius relationship with temp and volt, one can follow steps analogous to those outlined in Sect. 22.3.4. Using the dielectric strength (degradation path) model at time t, $\mathcal{D}(t) = \delta_0 \left[\mathcal{R}(\text{temp}, \text{volt}) \times t\right]^{1/\gamma_1}$. Using (22.8) with $X = \log(\text{volt})$, we obtain

$$\mathcal{R}(\text{temp}, \text{volt}) = \gamma_0 \times \exp\left(\frac{-E_\text{a}}{k_\text{B} \times \text{temp K}}\right) \times \exp\left[\gamma_2 \log(\text{volt}) + \frac{\gamma_3 \log(\text{volt})}{k_\text{B} \times \text{temp K}}\right] .$$

Again, failure occurs when the dielectric strength crosses the applied voltage stress, that is, $\mathcal{D}(t) = \text{volt}$. This occurs at time

$$T(\text{temp}, \text{volt}) = \frac{1}{\mathcal{R}(\text{temp}, \text{volt})} \left(\frac{\text{volt}}{\delta_0}\right)^{\gamma_1} .$$

From this, one computes

$$\begin{aligned}\mathcal{AF}(\text{temp, volt}) &= \frac{T(\text{temp}_\text{U}, \text{volt}_\text{U})}{T(\text{temp, volt})} \\ &= \exp[E_\text{a}(x_{1U} - x_1)] \\ &\quad \times \left(\frac{\text{volt}}{\text{volt}_\text{U}}\right)^{\gamma_2 - \gamma_1} \\ &\quad \times \{\exp[x_1 \log(\text{volt}) \\ &\quad - x_{1U} \log(\text{volt}_\text{U})]\}^{\gamma_3}.\end{aligned}$$

where $x_{1\text{U}} = 11605/(\text{temp}_\text{U}\,\text{K})$ and $x_1 = 11605/(\text{temp K})$. When $\gamma_3 = 0$, there is no interaction between temperature and voltage. In this case, $\mathcal{AF}(\text{temp, volt})$ can be factored into two terms, one that involves temperature only and another term that involves voltage only. Thus, if there is no interaction, the contribution of temperature (voltage) to acceleration is the same at all levels of voltage (levels of temperature).

Temperature–Current Density Acceleration Models

d'Heurle and *Ho* [22.15] and *Ghate* [22.16] studied the effect of increased current density (A/cm^2) on electromigration in microelectronic aluminum conductors. High current densities cause atoms to move more rapidly, eventually causing extrusion or voids that lead to component failure. ATs for electromigration often use increased current density and temperature to accelerate the test. An extended Arrhenius relationship could be appropriate for such data. In particular, when T has a log-location-scale distribution, then (22.10) applies with $x_1 = 11605/\text{temp K}$, $x_2 = \log(\text{current})$. The model with $\beta_3 = 0$ (without interaction) is known as Black's equation (*Black* [22.17]).

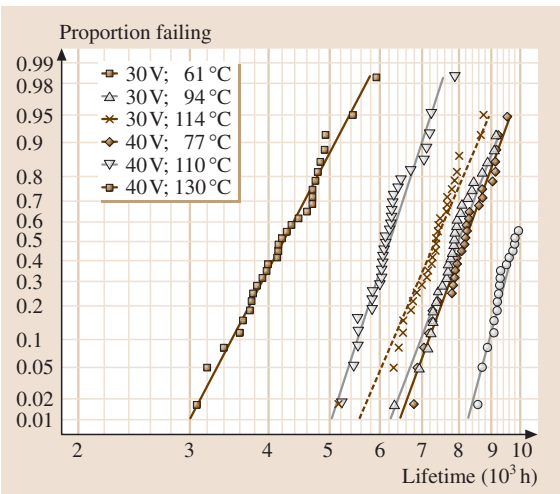

Fig. 22.4 LED device data. Lognormal multiple probability plot with lognormal ML fits for each combination of voltage/temperature

Example 22.4: Light Emitting Device (LED) Example. A degradation study on a light emitting device LED was conducted to study the effect of current and temperature on light output. A unit was said to have failed if its output was reduced to 60% of its initial value. Two levels of current and six levels of temperature were used in the test. Figure 22.4 is a probability plot of lifetimes for each combination of current and temperature. The plot suggests that the lognormal distribution is an appropriate distribution for lifetime and that increasing either temperature or current results in shorter device life.

Temperature–Humidity Acceleration Models

Relative humidity is another environmental variable that can be combined with temperature to accelerate corrosion or other chemical reactions. Examples of applications include paints and coatings, electronic devices and electronic semiconductor parts, circuit boards, permalloy specimens, foods, and pharmaceuticals. Although most ALT models that include humidity were derived empirically, some humidity models have a physical basis. For example, *Gillen* and *Mead* [22.18] and *Klinger* [22.19] studied kinetic models relating aging with humidity. *LuValle* et al. [22.20] provided a physical basis for studying the effect of humidity, temperature, and voltage on the failure of circuit boards. See *Boccaletti* et al. [22.21], *Nelson* ([22.1], Chapt. 2) *Joyce* et al. [22.22], *Peck* [22.23], and *Peck* and *Zierdt* [22.24] for ALT applications involving temperature and humidity.

The extended Arrhenius relationship (22.10)) applied to ALTs with temperature and humidity uses $x_1 = 11605/\text{temp K}$, $x_2 = \log(\text{RH})$, and $x_3 = x_1 x_2$, where RH is a proportion denoting relative humidity. The case when $\beta_3 = 0$ (no temperature–humidity interaction) is known as Peck's relationship and was used by Peck [22.23] to study failures of epoxy packing. Klinger [22.19] suggested the term $x_2 = \log[\text{RH}/(1 - \text{RH})]$ instead of $\log(\text{RH})$. This alternative relationship is based on a kinetic model for corrosion.

The Eyring Model

Fundamental work on the relationship between reaction rates and temperature, in combination with other variables, was done by Eyring in a number of important works (*Eyring*, *Gladstones*, and *Laidler* [22.25] and

Eyring [22.26]). The Eyring model is the same as the extended Arrhenius model described in this section, except that it has an additional factor $g(\text{temp K})$ outside of the exponential in (22.8). Usually, $g(\text{temp K}) = (\text{temp K})^p$ is used. For the purposes of using a fitted acceleration model to predict life at use conditions, for any practical values of the model parameters, this extra factor and estimating p along with E_a have no perceptible effect on the prediction. Thus the simpler Arrhenius model is what is generally used in practice. See *Meeker* and *Escobar* ([22.3], Sect. 18.3.2) and the above references for more information on the Eyring model.

22.3.6 Guidelines and Issues for Using Acceleration Models

The main objective of AT is to collect data at high levels of accelerating variables and extrapolate the results to use conditions. This section provides some guidelines and lists some common issues that arise in fitting acceleration models to ALT data.

- Whenever possible, the acceleration model should have a basis in physical or chemical theory. A careful review of previous theoretical and empirical work will often shed light on which environmental factors and degradation processes are relevant to a failure mechanism. It is highly recommended that a group of experts oversee the entire project of planning, collecting and analyzing AT data. This group should include experts with a clear understanding of the mechanical, physical and chemical nature of how the product degrades and eventually fails. This team should also include someone who is knowledgeable of the statistical aspects of planning life tests and analyzing the resulting data.
- ATs often assume a relatively simple failure mechanism or degradation process. It is possible at high levels of an accelerating variable to introduce new failure mechanisms. Acceleration could also alter other environmental factors that affect the failure mechanism. For example, *Meeker* and *Escobar* ([22.3], page 526) pointed out that ALT tests of circuit packs at higher temperatures reduced humidity, causing fewer failures than expected. Potential scenarios like these should be considered for both planning and modeling ATs.
- The main difficulty with extrapolation in ATs is that there is rarely sufficient data at lower levels of the accelerating variable to verify that the acceleration model for the failure mechanism still holds at use conditions. Thus, a good test plan minimizes the amount of acceleration while providing a statistically efficient description of the failure mechanism at use conditions. There is a large amount of work that has been done on ALT planning. For an overview of this work, see, for example, *Nelson* ([22.1], Chapt. 6) and *Meeker* and *Escobar* ([22.3], Chapt. 20 and Sect. 22.5).
- The statistical analysis of ALT data depends importantly on the acceleration model and distribution assumptions. A sensitivity analysis should be conducted to study how results (e.g., quantile and failure probability estimates) vary with changes in the assumed model and distribution. The results of such sensitivity analyses can help decision-makers understand whether model assumptions are conservative or not.

22.4 Analysis of Accelerated Life Test Data

This section discusses the statistical analysis of ALT data. First, we outline a useful strategy to follow when choosing and fitting a model to ALT data and assessing the adequacy of the fit. Then we illustrate the proposed strategy with several different ALT applications having either one or two accelerating variables.

22.4.1 Strategy for ALT Data Analysis

This section outlines some guidelines for analyzing ALT data. Suppose that groups of data were collected under several individual conditions (levels or level combinations of the accelerating variables).

1. Make a scatter plot of the lifetimes versus the explanatory variable(s) to help in the identification of an appropriate relationship or model.
2. For each individual condition, make a probability plot (*Meeker* and *Escobar*, [22.3], Chapts. 6 and 21) of the data under candidate distributions and obtain ML estimates of the parameters. A distribution provides a good fit if the plotted points fall roughly along a straight line. Check the constant-σ assump-

tion visually by comparing the slopes of the lines in the probability plots and statistically by comparing the estimates of σ.

3. Fit a model constraining σ to be the same at each level and compare with the unconstrained model in Step 3. This provides the basis for a formal test of constant σ.
4. Based on the previous steps, choose and fit and overall model (distribution and acceleration model).
5. Compare the overall model fit in Step 4 to the common-σ model fit in Step 3. Large discrepancies between these two models suggest an inadequate fit for the overall model.
6. Use diagnostics such as residual plots to assess the fit of the overall model and to check the model assumptions.

22.4.2 Data Analysis with One Accelerating Variable

This section describes the analysis of several different kinds of ALT data sets, following and illustrating the ALT analysis strategy outlined in Sect. 22.4.1.

ALT Data Scatter Plot

The first step is to make a scatter plot of the data and study how the accelerating variable affects the lifetime. Use a different plotting symbol to indicate censored observations.

Example 22.5: Scatter Plot of the GAB Insulation Data. Example 22.2 described a generator armature bar insulation ALT. A scatter plot of the data, given in Fig. 22.2, suggests a downward trend in lifetime as voltage stress is increased. There was heavy censoring at the lower voltage stresses. In particular, 8 out of 12 units failed at 190 V/mm and none of the 12 units failed at 170 V/mm.

Multiple Probability Plots at Individual Conditions of the Accelerating Variable

For each level (individual condition) of the accelerating variable(s), compute a nonparametric estimate of the fraction failing as a function of time and plot it on probability paper for a suggested lifetime distribution. The distribution adequately describes the data if, for each individual condition, the points lie close to a straight line. ML can be used to fit a line through the points at each level. A multiple probability plot showing these nonparametric estimates and fitted lines for all of the levels of the accelerating variable provides a convenient visual assessment of the constant-σ assumption. If the assumption is reasonable, the lines will be approximately parallel. Repeat this for different lifetime distributions.

Example 22.6: Probability Plots at Individual Conditions for the GAB Insulation Data. Figures 22.5 and 22.6 give lognormal and Weibull multiple probability plots, respectively, for the GAB insulation data. There is nothing plotted for 170 V/mm because there were no failures at this level of voltage stress. The points for each voltage stress level fall roughly along a straight line, and the lines appear to be reasonably parallel (but more parallel with the Weibull distribution). It appears that

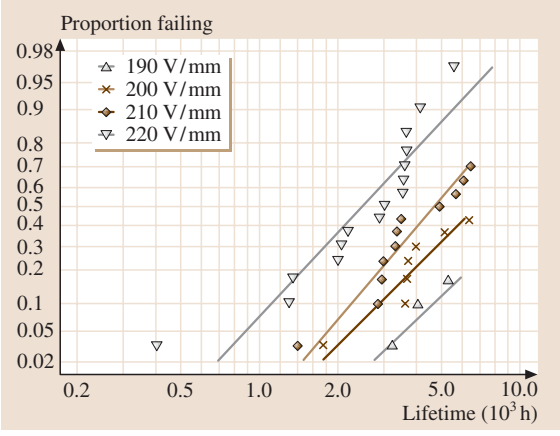

Fig. 22.5 GAB insulation data. Lognormal multiple probability plot with lognormal ML fits for each level of voltage stress

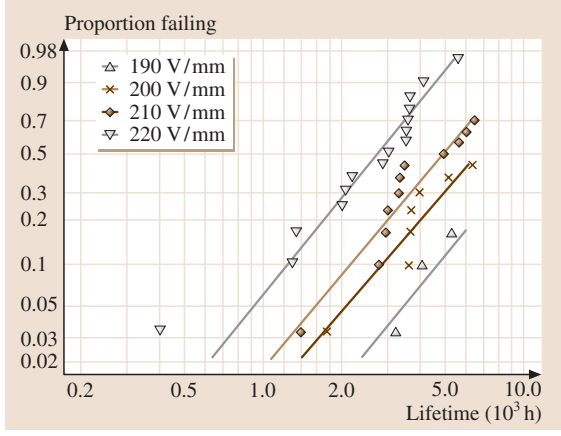

Fig. 22.6 GAB insulation data. Weibull multiple probability plot with Weibull ML fits for each level of voltage stress

Table 22.2 GAB insulation data. Weibull ML estimates for each voltage stress

	Parameter	ML estimate	Standard error	Normal-approximation 95% confidence interval
190	μ	2.49	0.44	[1.63, 3.35]
	σ	0.42	0.23	[0.14, 1.26]
200	μ	2.07	0.20	[1.68, 2.45]
	σ	0.45	0.16	[0.23, 0.89]
210	μ	1.74	0.13	[1.49, 2.00]
	σ	0.44	0.11	[0.26, 0.73]
220	μ	1.17	0.11	[0.94, 1.39]
	σ	0.42	0.09	[0.28, 0.64]

The individual maximum log likelihoods were $\mathcal{L}_{190} = -12.31$, $\mathcal{L}_{200} = -22.09$, $\mathcal{L}_{210} = -27.54$, and $\mathcal{L}_{220} = -25.05$. The total log likelihood for this model is $\mathcal{L}_1 = -86.99$

both the Weibull and the lognormal distributions provide adequate descriptions of the GAB data. At each level of voltage stress, the Weibull distribution is fitted to the data, and estimates of μ and σ were computed by using the method of ML. Table 22.2 gives the ML estimates of μ and σ for each level of voltage stress. Table 22.2 also provides approximate standard errors and normal-approximation-based confidence intervals. The lines drawn in Fig. 22.6 represent the ML estimates of the individual CDFs (fraction failing) at each level of voltage stress.

The ML estimates of σ for all levels of voltage stress are similar. The similarities are reflected in the near-parallel CDF lines drawn in Fig. 22.6. Although details are not shown here, the maximum total log likelihood value achieved by fitting Weibull distributions with common σ (the location parameters are allowed to float) to each individual condition is $\mathcal{L}_2 = -87.01$ which is very close to the total log-likelihood $\mathcal{L}_1 = -86.99$ obtained from fitting separate Weibull distributions. This suggests that it is reasonable to assume that σ is constant across voltage stresses.

Maximum Likelihood Estimate of the ALT Model

The inverse power relationship is often used to relate the lifetime distribution of a dielectric to voltage stress. Suppose that $T(\text{volt})$, the lifetime at volt, has a log-location-scale distribution with parameters (μ, σ) and that σ does not depend on volt. Under the inverse power relationship, $\mu = \beta_0 + \beta_1 x$ where $x = \log(\text{volt})$. Fitting the model to data is accomplished by computing estimates for the parameters β_0, β_1, and σ.

Example 22.7: Maximum Likelihood Estimate of the Inverse Power Model for the GAB Insulation Data. The results of fitting the inverse power relationship Weibull model to the data are summarized in Table 22.3. A likelihood ratio test comparing with the constant-σ/floating-μ model allows a formal assessment of whether the inverse power relationship is consistent with the data. Fitting the inverse power relationship with constant σ also allows extrapolation to the use level of 120 V/mm.

Suppose that model B is obtained by imposing constraints on the parameters of model A (e.g., the constraint that the location parameters at different levels of voltage stress are related by the inverse power relationship). For $i = \text{A, B}$, let $\mathcal{L}_i$ be the maximum total log likelihood achieved by fitting model i to the data. If model B is the correct model, in large samples, the likelihood ratio statistic $\mathcal{W} = 2 \times (\mathcal{L}_\text{A} - \mathcal{L}_\text{B})$ has a χ^2_ν distribution with degrees of freedom ν equal to the difference between the number of estimated model parameters in the two models. Large values of $\mathcal{W}$ indicate evidence

Table 22.3 GAB insulation data. ML estimates for the inverse power relationship Weibull regression model

Parameter	ML estimate	Standard error	Normal-approximation 95% confidence interval
β_0	53.39	9.46	[34.84, 71.93]
β_1	−9.68	1.77	[−13.14, −6.21]
σ	0.44	0.06	[0.33, 0.58]

The maximum log likelihood for this model is $\mathcal{L}_3 = -87.72$

against the constrained model model B, relative to the unconstrained model A. The difference is statistically important at the α level if $\mathcal{W} \geq \chi^2_{(1-\alpha;\nu)}$ where $\chi^2_{(1-\alpha;\nu)}$ is the $(1-\alpha)$ quantile of the χ^2_ν distribution.

For the GAB insulation data, model A is the (unconstrained) set of Weibull distributions with common σ (five parameters), and model B is the (constrained) inverse power relationship Weibull model (three parameters). Then $\mathcal{L}_A = \mathcal{L}_2 = -87.01$, $\mathcal{L}_B = \mathcal{L}_3 = -87.72$, and $\mathcal{W} = 1.42 < \chi^2_{(0.95;2)} = 5.99$. Thus, the difference between the fits is not statistically important at the 0.05 level and the data do not provide evidence against model B.

The maximum log likelihood value attained with the lognormal distribution is -89.52, which is close to $\mathcal{L}_3 = -87.72$ for the Weibull distribution. Again, as noted earlier with the probability plots, both the Weibull and lognormal models fit the data well.

Figure 22.7 is a probability plot showing the ML fit of the inverse power relationship Weibull model to the data. It also gives the ML estimate of the fraction failing at use conditions $\text{volt}_U = 120\,\text{V/mm}$. The dashed lines give pointwise normal-approximation 95% confidence intervals for the fraction failing at use conditions. Conversely, this plot can be used to obtain an estimate and an approximate confidence interval for specified quantiles at use conditions. Figure 22.8 is a scatter plot of the GAB data with ML estimates of the 0.1, 0.5, and 0.9 quantiles at all levels of voltage stresses between 120 and 220 V/mm. The horizontal line indicates the censoring time at 6480 h. Densities (smallest extreme-value densities because time is plotted on a log scale) are shown at the voltage stresses in the experiment as well as at the use condition of 120 V/mm. Figure 22.8 suggests that it is unlikely that one would observe any failures below 170 V/mm during the ALT experiment.

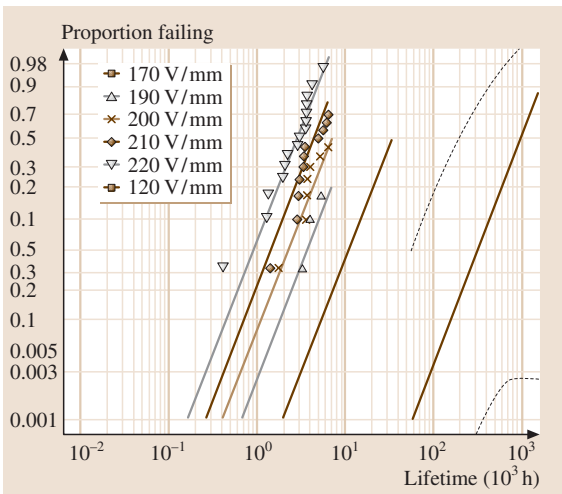

Fig. 22.7 GAB insulation data. Weibull multiple probability plot depicting the inverse power relationship Weibull regression model ML fit

Assessing Statistical Uncertainty

An estimate of the variance–covariance matrix for the ML estimates $\hat{\boldsymbol{\theta}} = (\hat{\beta}_0, \hat{\beta}_1, \hat{\sigma})'$ is

$$\widehat{\sum}_{\hat{\boldsymbol{\theta}}} = \begin{pmatrix} 89.52 & -16.73 & 0.27 \\ -16.73 & 3.13 & -0.05 \\ 0.27 & -0.05 & 0.004 \end{pmatrix} . \qquad (22.11)$$

The elements of this matrix are used to compute normal-approximation confidence intervals, as described in Example 22.9. This matrix is usually available (at least as an option) as output from computer software and is useful for computing the variance of functions of the parameters (e.g., quantiles and fraction failing estimates) that may be of interest. In modern software for life data analysis, however, such computations are easy to request and printing the variance–covariance matrix is often suppressed by default.

Diagnostics and Assessing Fit of ALT Model to Data

Plots like Figs. 22.7 and 22.8 can be used to assess the fit of a model to a set of data. Graphical analyses

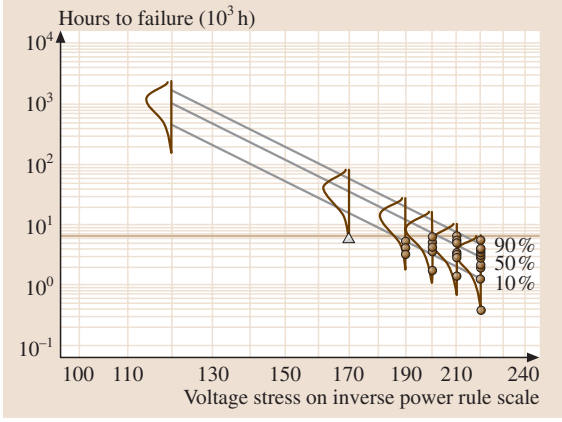

Fig. 22.8 GAB insulation data. Scatter plot showing hours to failure versus voltage stress (log–log scales) and the inverse power relationship Weibull regression model fit. Censored observations are indicated by Δ

of the standardized residuals, $\exp[\log(t) - \hat{\mu}]/\hat{\sigma}$, provide additional diagnostics for judging model adequacy. Residuals can be plotted against the order of the test runs, fitted values, and levels of explanatory variables that are or are not in the fitted model. It is necessary to take into account the amount of censoring during interpretation. An overall assessment of the distributional assumption can be obtained by using a probability plot of the residuals.

Example 22.8: Residuals Plots for the Inverse Power Relationship Weibull Model Fit to the GAB Insulation Data. Figure 22.9 plots residuals versus fitted values. The vertical axis shows the standardized residuals. The horizontal lines are the 0.05, 0.50, and 0.95 quantiles of a standard exponential distribution (e.g., $-\log(1-0.95) = 2.996$ is the 0.95 quantile of this distribution). For the Weibull distribution, the residuals should have an approximate standard Weibull ($\mu = 0, \sigma = 1$) distribution (which is left-skewed). Thus, the Weibull distribution is appropriate if the residuals have a long lower tail. At 210 V/mm, where all of the test units failed, the residuals (first column of points in Fig. 22.9) indicate a left-skewed distribution about the center line, indicating no lack of fit of the Weibull distribution. The interpretation of the residuals is not as simple for the levels 170, 190, 200, and 210 V/mm (the last four columns of points in Fig. 22.9) because all of these levels resulted in some censored observations. The triangles (△) in Fig. 22.9 indicate lower bounds for residuals for these censored observations (i. e., the actual unobserved residuals corresponding to these points would be larger than the plotted triangles). With this in mind, there is no strong evidence of lack of fit of the Weibull distribution at these levels. Figure 22.10 is a Weibull probability plot of the residuals for all failures. The residuals fall close to a straight line, which suggests that there is no problem with the Weibull assumption.

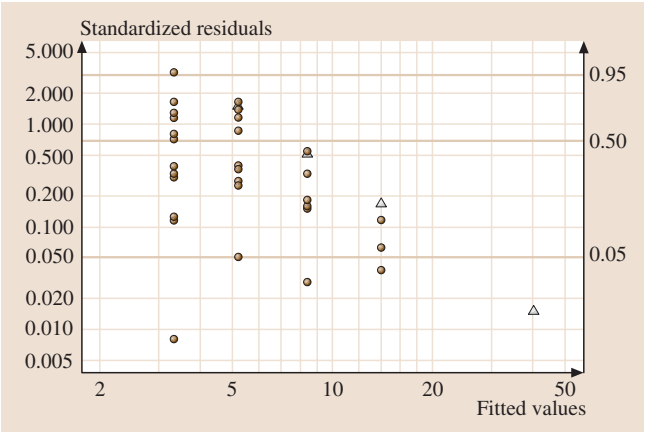

Fig. 22.9 GAB insulation data. Plot of standardized residuals versus fitted values for the inverse power relationship Weibull regression model. Censored observations are indicated by Δ

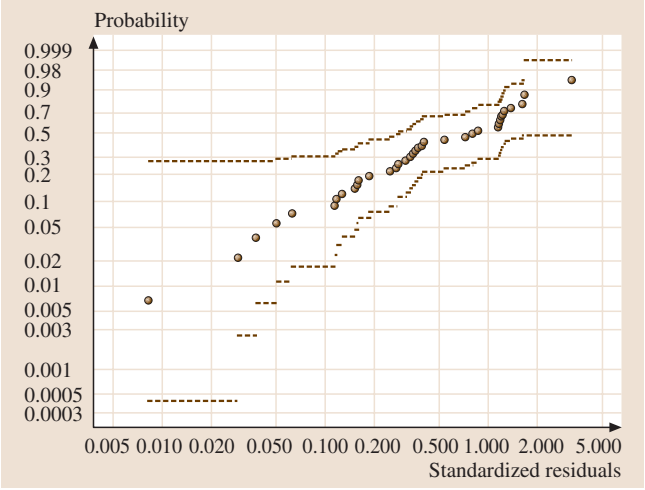

Fig. 22.10 GAB insulation data. Weibull probability plot of the standardized residuals from the inverse power relationship Weibull regression model fit

Estimation at Use Conditions and Sensitivity to Model Assumptions

It is important to quantify the statistical uncertainty in estimates from an ALT. Here, we illustrate the computation of normal-approximation confidence intervals for quantiles. See Sect. 17.4.2 of *Meeker* and *Escobar* [22.3] for a more general discussion of the methodology. The following example also contains a sensitivity analysis of the estimates with respect to the assumed distribution.

Example 22.9: ML Estimates and Confidence Intervals for Quantiles for the GAB Insulation Data Life Distribution. For the GAB experiment, it was of interest to estimate the 0.01 and 0.05 quantiles of insulation life at the 120 V/mm use condition. The ML estimate of the location parameter at 120 V/mm, computed from the ML estimates for the parameters in Table 22.3, is

$$\hat{\mu} = \hat{\beta}_0 + \hat{\beta}_1 x = 53.39 - 9.68 \log(120) = 7.07 \,.$$

The ML estimate of the log p quantile is

$$\begin{aligned} \log(\widehat{t_p}) &= \hat{\mu} + \log[-\log(1-p)]\,\hat{\sigma} \\ &= 7.07 + \log[-\log(1-p)] \times 0.44 \end{aligned}$$

Table 22.4 GAB insulation data. Quantiles ML estimates at 120 V/mm

Distribution	Quantile	ML estimate	Normal-approximation 95% confidence interval
Weibull	t_{01}	154.6×10^3 h	[26.4, 907.4] $\times 10^3$ h
		17.7 y	[3.0, 103.6] y
	t_{05}	317.0×10^3 h	[51.4, 1953.0] $\times 10^3$ h
		36.2 y	[5.9, 223.0] y
Lognormal	t_{01}	254.4×10^3 h	[43.4, 1492.9] $\times 10^3$ h
		29.1 y	[5.0, 170.0] y
	t_{05}	390.8×10^3 h	[63.4, 240.9] $\times 10^3$ h
		44.6 y	[7.0, 27.5] y

with an estimated standard error $\widehat{\text{se}}_{\log(\widehat{t}_p)} = \sqrt{\widehat{\text{Var}}_{\log(\widehat{t}_p)}}$ $= \sqrt{\boldsymbol{c}' \widehat{\sum}_{\hat{\boldsymbol{\theta}}} \boldsymbol{c}}$, where $\mathbf{c} = \{1, \log(\text{volt}), \log[-\log(1-p)]\}'$ and $\widehat{\sum}_{\hat{\boldsymbol{\theta}}}$ is given in (22.11). A $100(1-\alpha)\%$ normal-approximation confidence interval for t_p is

$$\exp\left[\log(\widehat{t}_p) \pm z_{(1-\alpha/2)} \times \widehat{se}_{\log(\widehat{t}_p)}\right] = \widehat{t}_p \exp\left(\pm z_{(1-\alpha/2)} \times \widehat{se}_{\log(\widehat{t}_p)}\right) ,$$

where z_γ is the γ quantile of the standard normal distribution. Table 22.4 gives the ML estimates and 95% confidence intervals for the 0.01 and 0.05 quantiles at 120 V/mm. the data that was almost as good as the fit with the Weibull distribution. Table 22.4 also includes quantile estimates for the lognormal distribution. Although the differences between the Weibull and lognormal distribution point estimates may be judged to be large, the confidence interval for the quantile under one distribution contains the point estimate under the other. The lognormal distribution quantile estimates are optimistic relative to those for the Weibull distribution.

22.5 Further Examples

This section illustrates the use of the statistical methods, outlined in Sect. 22.4, to various other ALT applications. The examples show the fit of ALT models to interval-censored data and reliability data with two or

Table 22.5 IC device data

Temperature (°C)	Time Bounds (h)		Frequency	Censoring
	Lower	Upper		
150	788		1	Right
150	2304		49	Right
175	788		1	Right
175	2304		49	Right
200	788		1	Right
200	2304		49	Right
250	384	788	1	Interval
250	788		1	Right
250	1536	2304	6	Interval
250	2304		42	Right
300	96	192	1	Interval
300	192	384	6	Interval
300	384	788	20	Interval
300	384		2	Right
300	788	1536	16	Interval
300	1536		5	Right

more explanatory variables. These examples illustrate a wider (but not exhaustive) range of data types that arise in practice, provide more insight into how to develop ALT models, address the goals and objectives of the experiment, and study the effect of model assumptions on these aims (sensitivity analyses).

22.5.1 Analysis of Interval Censored ALT Data

Interval-censored data are common in ALT studies. Constraints on resources limit the frequency of inspection times in tests. As a consequence, engineers often fail to observe failures instantaneously, and inspection times serve as bounds for lifetimes.

Example 22.10: Analysis of Integrated Circuit Device ALT Data. Table 22.5 gives the results of an ALT for an integrated circuit (IC) device at five different levels of junction temperature. Because the diagnostic testing of each device was expensive, each unit could only be inspected a few times during the ALT. Consequently, an observation was either interval-censored (bounds for lifetime were recorded) or right-censored (lower bound for lifetime was recorded). The engineers chose inspection times that were approximately equally spaced in log time. Tests were conducted at 150, 175, 200, 250, and 300 °C on a total of 250 devices (50 at each level of temperature).

The objectives of the ALT was to quantify the long-term reliability of the ICs and to estimate the effective activation energy of the failure mechanism. In particular, the engineers involved in the study wanted to assess the hazard rate and the fraction failing by 100 000 hours at the use junction temperature of 100 °C.

Figure 22.11 is a lognormal probability plot of the data at individual conditions. There are no plots for 150, 175, 200 °C because there were no failures at these levels of temperature. The ML results for estimating the lognormal parameters at individual temperatures are given in Table 22.6. The fitted CDF lines drawn in the plot appear to be reasonably parallel. Also, the ML estimates of σ and corresponding confidence intervals do not indicate evidence against the constant-σ assumption across temperature levels. Table 22.7 gives the ML results of fitting an Arrhenius lognormal model to the IC device data. An estimate of the effective activation energy is $\widehat{E}_a = \widehat{\beta}_1 = 0.94$.

Figure 22.12 is a probability plot depicting the ML fit of the Arrhenius lognormal model to the data. It also gives the ML estimate of the fraction failing at $\text{temp}_U = 100\,°\text{C}$ with pointwise normal-approximation 95% confidence intervals. Figure 22.12 plots the ML estimates of the 0.1, 0.5, and 0.9 quantiles with the data for temperatures between 100 and 300 °C. Even though there is a large amount of statistical uncertainty, Figs. 22.12 and 22.13 both suggest that it is very unlikely that failures would occur before 100 000 hours at $\text{temp}_U = 100\,°\text{C}$.

Observing failures at two or more levels of the accelerating variable is necessary to estimate the parameters of the Arrhenius relationship. There are situations in which the activation energy E_a is specified, based

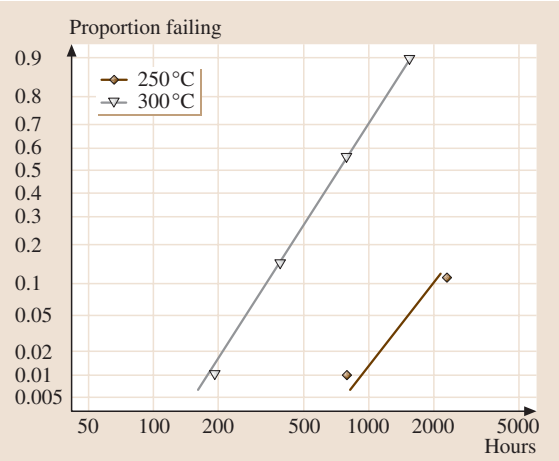

Fig. 22.11 IC device data. Lognormal multiple probability plot with individual lognormal ML fits for each temperature

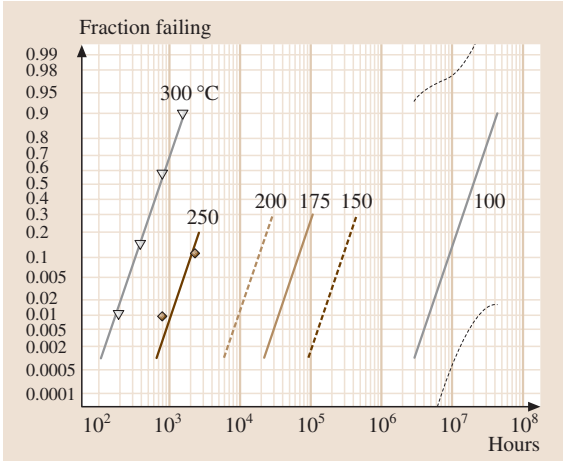

Fig. 22.12 IC device data. Lognormal multiple probability plot depicting the Arrhenius lognormal regression model ML fit

Table 22.6 IC device data. Lognormal ML estimates for each temperature

Temperature (°C)	Parameter	ML estimate	Standard error	Normal-approximation 95% confidence interval
250	μ	8.54	0.34	[7.87, 9.22]
	σ	0.74	0.25	[0.38, 1.43]
300	μ	6.58	0.20	[8.59, 9.36]
	σ	0.61	0.07	[0.48, 0.76]

The individual maximum log likelihoods were $\mathcal{L}_{250} = -26.11$ and $\mathcal{L}_{300} = -63.18$. The total log likelihood for this model is $\mathcal{L}_4 = -89.29$

Table 22.7 IC device data. ML estimates for the Arrhenius lognormal regression model

Parameter	ML estimate	Standard error	Normal-approximation 95% confidence interval
β_0	−12.45	1.95	[−16.26, −8.63]
β_1	0.94	0.09	[0.76, 1.12]
σ	0.62	0.07	[0.50, 0.77]

The maximum log likelihood for this model is $\mathcal{L}_5 = -89.45$

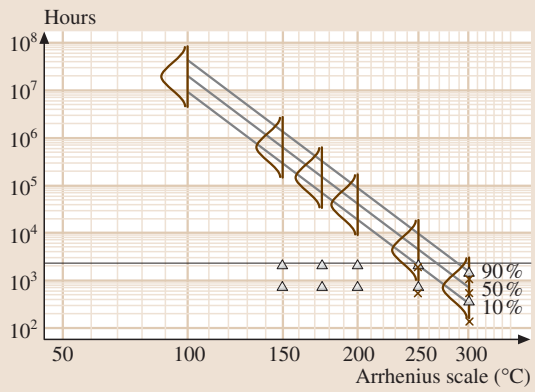

Fig. 22.13 IC device data. Scatter-plot interval midpoints failure versus °C (on an Arrhenius scale) and the Arrhenius lognormal regression model fit. Censored observations are indicated by Δ

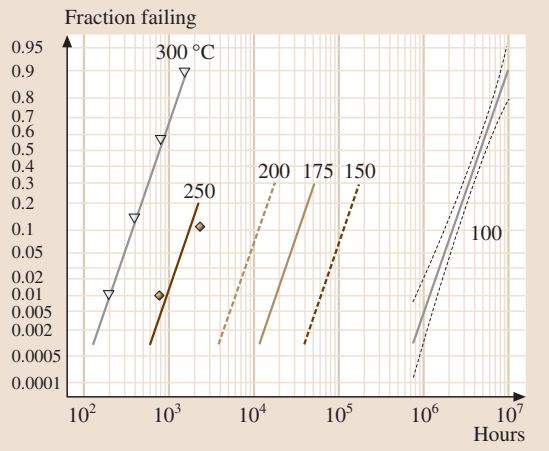

Fig. 22.14 IC device data. Lognormal probability plot showing the Arrhenius lognormal model ML estimates and 95% confidence intervals for $F(t)$ at 100 °C given $E_a = 0.8$ eV

on prior experience with the product, in which case only one temperature level with failures may suffice for estimation. For example, MIL-STD-883 [22.27] gives guidelines for conducting reliability demonstrations tests when E_a is given.

Example 22.11: Analysis of the IC Device Data when the Activation Energy is Given. Figure 22.14 is similar to Fig. 22.12, but obtained with $E_a = 0.8$ eV given. Now, the confidence intervals for the fraction failing at $\text{temp}_U = 100$ °C are much narrower than when E_a had to be estimated. This difference reflects a tremendous, probably unreasonable, gain in precision. Because there will be doubt about the actual value of E_a, one must exercise caution in interpreting such an analysis. Varying $\beta_1 = E_a$ over some plausible range of values provides a useful sensitivity analysis. Also a Bayesian analysis could be used when the uncertainty on E_a can be specified by a probability distribution (see *Meeker* and *Escobar* [22.3], Sect. 22.2).

22.5.2 Analysis of Data From a Laminate Panel ALT

A sample of 125 circular-holed notched specimens of a carbon eight-harness-satin/epoxy laminate panel were

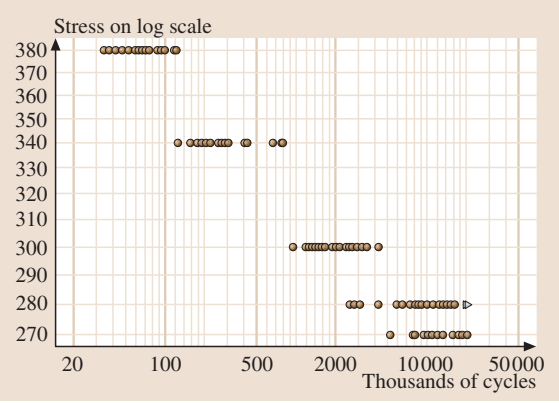

Fig. 22.15 Laminate panel data. Log–log scatter plot of life versus stress

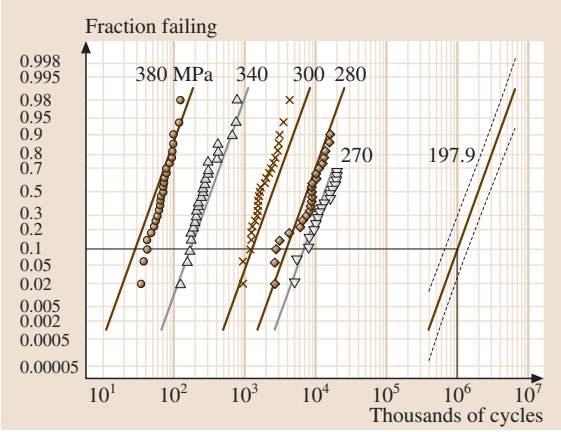

Fig. 22.16 Laminate panel data. Lognormal probability plot showing the inverse power relationship lognormal model ML fit and 95% confidence intervals for $F(t)$ at 197.9 MPa

subjected to a cyclic four-point out-of-plane bending at several levels of stress, measured in MPa. The data are from *Shimokawa* and *Hamaguchi* [22.28]. In these tests, final specimen fracture and fiber fracture occurred simultaneously. The lifetime of a specimen is the number of cycles to fracture. Figure 22.15 is a log–log scatter plot of the data. Note that the response (thousands of cycles) is plotted on the horizontal axis (the usual convention in the fatigue-fracture literature). Ten specimens were right-censored (two at 280 MPa and eight at 270 MPa). The goals of experiment were to estimate the relationship between life and stress (or the S–N curve) and a safe level of stress for a given life quantile. Figure 22.16 is a multiple lognormal probability plot of the data. The lognormal distribution appears to be appropriate here. Figure 22.15 indicates a strong linear correlation between log life and log stress. These plots suggest fitting a inverse power relationship lognormal model to the data.

Example 22.12: ML Estimate of the Inverse Power Relationship Lognormal Model for the Laminate Panel Data. For the inverse power relationship lognormal model, the parameters are $\mu = \beta_0 + \beta_1 x$ and σ, where $x = \log(\text{Stress})$. Table 22.8 gives the results of the ML estimation of β_0, β_1 and σ with the laminate panel data.

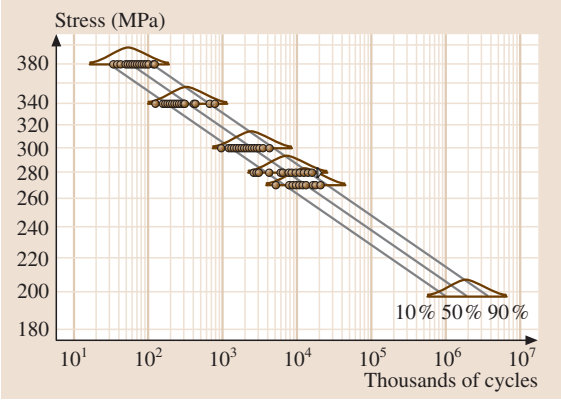

Fig. 22.17 Laminate panel data. Scatter-plot showing cycles to failure versus MPa (on a log scale) and the inverse power relationship lognormal regression model ML fit. Censored observations are indicated by Δ

Estimates of the fraction failing at the individual stress levels of the experiment are drawn in Fig. 22.16. Figure 22.17 is a scatter plot of the data with ML estimates of the 0.1, 0.5, and 0.9 quantiles. The confidence intervals for the life distribution at use conditions in this

Table 22.8 Laminate panel data. ML estimates for the inverse power relationship lognormal regression model

Parameter	ML estimate	Standard error	Normal-approximation 95% confidence interval
β_0	99.36	2.14	[95.16, 103.55]
β_1	−16.05	0.37	[−16.78, −15.32]
σ	0.52	0.04	[0.46, 0.60]
The maximum log likelihood for this model is $\mathcal{L}_6 = -898.3$			

example are much narrower, when compared to those for the IC device example shown in Fig. 22.12. This is because there is less censoring and less relative extrapolation in the inference for the laminate panel data. The median (0.50 quantile) life line in Fig. 22.17 provides the estimate of the S–N curve that was of interest to the engineers.

Example 22.13: Estimate of a Safe-Level Stress for the Laminate Panel Data. The engineers wanted to estimate a safe level of stress at which no more than 10% of the population of laminate panels would fail before 1 000 000 cycles. This involves determining the stress level at which the 0.10 quantile is 1 000 000 cycles. At any stress below this safe level of stress, the population fraction failing before 1 000 000 cycles will be more than 0.10. Using the inverse power relationship lognormal model, the safe stress level is

$$\text{safe stress} = \exp\left\{\left[\log\left(10^6\right) - 99.36 - \Phi_{\text{nor}}^{-1}(0.1) \times 0.52\right] / (-16.05)\right\} = 197.9\,\text{MPa}.$$

Figure 22.16 plots an estimate of the fraction failing (rightmost line) at this safe stress level. As seen in this plot, the stress 197.9 MPa is an extrapolation because the estimation is outside the range of the data. Of course, there is potential danger in making decisions based on this estimate, especially if the inverse power relationship lognormal model fails to hold below 270 MPa. Because the inverse power relationship is an empirical model and its use is based on past experience, it is important to perform a sensitivity analysis by computing safe-level estimates under alternative relationships. For example, the reciprocal relationship ($x = 1/\text{Stress}$) gives a model maximum log likelihood value of $\mathcal{L}_7 = -892.1$ which is larger than that from the inverse power relationship (indicating that the reciprocal model provides a better fit to the data). The estimate of the safe level of stress under the reciprocal relationship is equal to 216 MPa. This is larger (less conservative) than that under the inverse power relationship. Quantile estimates at a given stress level are also less conservative under the reciprocal relationship. That is, the estimates of life under the reciprocal relationship are longer than those under the inverse power relationship.

22.5.3 Analysis of ALT Data with Two or More Explanatory Variables

The single-variable analyses in Sects. 22.4, 22.5.1, and 22.5.2 can be extended to two or more variables (accelerated or otherwise). For example, ATs with multiple accelerating variables often use temperature in combination with humidity, pressure, and/or voltage. The goal of an AT may be to compare new and old product designs under different humidity levels, using temperature to accelerate the lifetimes. In this case, product design is a qualitative factor and the humidity range would mimic that seen in the actual application. This section illustrates the analysis of data from AT studies like these.

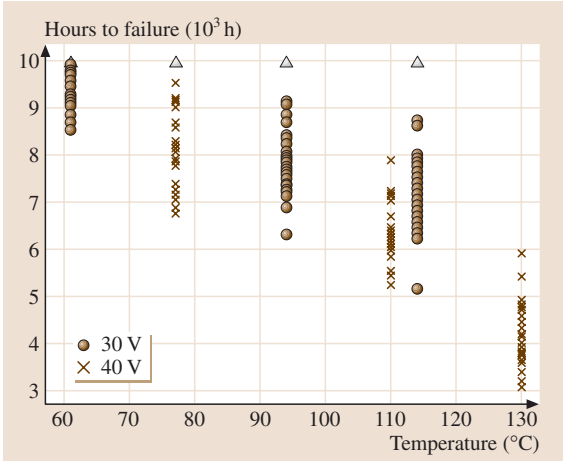

Fig. 22.18 LED device data. Scatter-plot showing hours to failure versus temperature with voltage indicated by different symbols. Censored observations are indicated by Δ

Example 22.14: Light Emitting Device Data with Accelerated Current and Temperature. Recall the LED device data from Example 22.4. The engineers were interested in the reliability of the LED at use conditions of 20 mA current and 40 °C temperature. Figure 22.18 plots the LED device data versus temperature for different levels of current. The plot suggests that failures occur earlier at higher levels of current or temperature.

The probability plot in Fig. 22.4 suggests that the lognormal distribution can be used to describe the lifetimes at each combination of current and temperature. Furthermore, because the lines are approximately parallel, it is reasonable to assume that σ is constant across individual conditions.

The inverse power (for current) and Arrhenius (for temperature) relationships are combined to model the effect that current and temperature have on lifetime. In particular, suppose that LED lifetime at volt and temp°C has a lognormal distribution with parameters μ given by

Main effects without interaction model:

$$\mu = \beta_0 + \beta_1 x_1 + \beta_2 x_2\,, \tag{22.12}$$

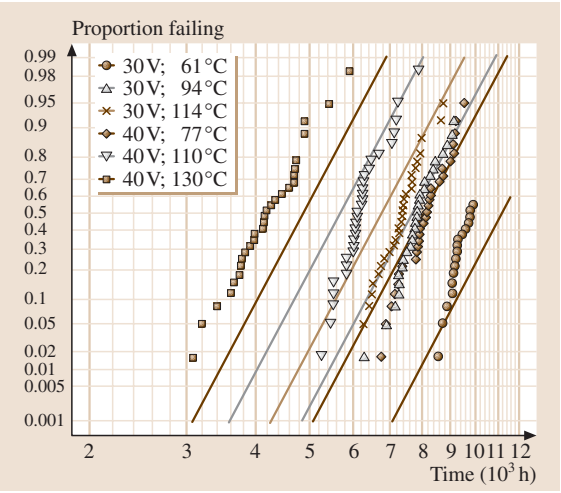

Fig. 22.19 LED device data. Multiple lognormal probability plot depicting the regression model (22.12) (without interaction) ML fit

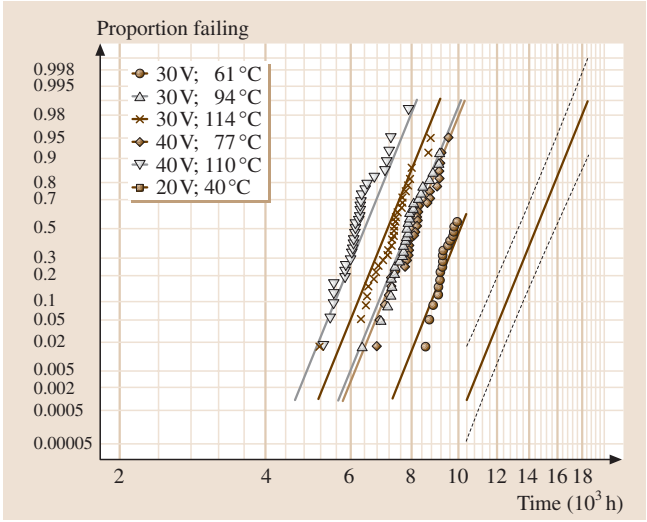

Fig. 22.20 LED device subset data. Multiple lognormal probability plot depicting the lognormal regression model (22.12) (without interaction) ML fit. The data at (40 V, 130 °C) were omitted

Main effects with interaction model:

$$\mu = \beta_0 + \beta_1 x_1 + \beta_2 x_2 + \beta_3 x_1 x_2 \,, \qquad (22.13)$$

where $x_1 = \log(\text{volt})$, $x_2 = 11605/(\text{temp K})$, and $\beta_2 = E_a$, and σ does not depend on $\boldsymbol{x}$. Fitting the model with interaction to the data resulted in life estimates at use conditions that were shorter than those observed at the more stressful test conditions. The engineers were sure this was wrong. It turned out that the incorrect estimates were caused by the interaction term in the model. The interaction term lead to nonlinearity in the response surface and resulted in a saddle point in the surface relating μ to the transformed explanatory variables. Because this model gave nonsense results, it will not be considered any further.

The fit of the main-effects model without interaction reveals strong lack of fit at the high-level combination of volt = 40 and temp°C = 130. Figure 22.19 is a probability plot depicting the ML estimates of the fraction failing as a function of time at individual conditions. Observe that the true fraction failing as a function of time is underestimated throughout the range of data at volt = 40 and temp°C = 130. If the main-effects model were physically appropriate, it appears that it may not hold when both volt and temp are at these high levels, probably because a new failure mechanism is excited at those extreme conditions.

Table 22.9 provides the ML results for the inverse-power Arrhenius lognormal model after deleting the

Table 22.9 LED device subset data. ML estimates for the lognormal regression models (22.12) and (22.13)

Model	Parameter	ML estimate	Standard error	Normal-approximation 95% confidence interval
Main effects without interaction	β_0	1.33	0.28	[0.78, 1.89]
	β_1	−0.46	0.06	[−0.58, −0.34]
	β_2	0.073	0.005	[0.063, 0.083]
	σ	0.11	0.07	[0.09, 0.12]
Main effects with interaction	β_0	13.54	4.20	[5.31, 21.78]
	β_1	−3.96	1.21	[−6.33, −1.60]
	β_2	−0.31	0.13	[−0.57, −0.05]
	β_3	0.11	0.04	[0.04, 0.18]
	σ	0.10	0.006	[0.09, 0.12]

The maximum log likelihood values are $\mathcal{L}_8 = -173.5$ (main effects without interaction) and $\mathcal{L}_9 = -169.5$ (main effects with interaction model)

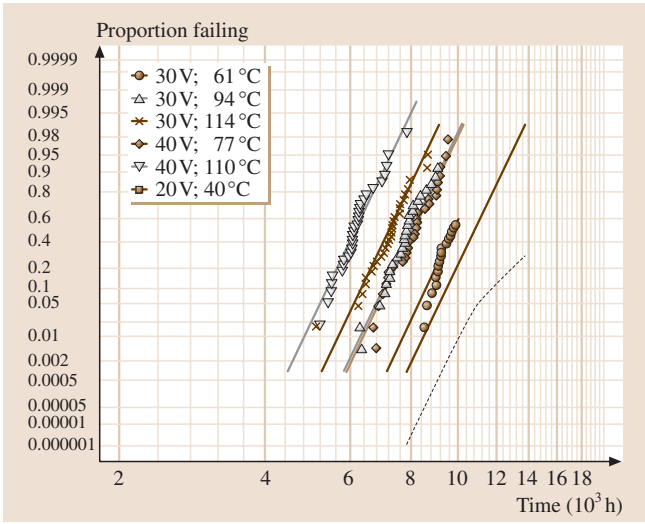

Fig. 22.21 LED device subset data. Multiple lognormal probability plot lognormal regression model (22.12) (with interaction) ML fit. The data at (40 V, 130 °C) were omitted

data at volt = 40 V and temp°C = 130 °C. Figure 22.20 shows a probability plot of the LED device subset data along with ML estimates of fraction failing as a function of time for the model without interaction.

Figure 22.20 is a lognormal probability plot of the LED device subset data along with ML estimates of fraction failing as a function of time. It also includes the ML estimate of the fraction failing as a function of time at the use conditions volt = 20 V and temp°C = 40 °C (the rightmost line). The dashed lines represent approximate 95% pointwise confidence intervals for the fraction failing as a function of time at these conditions. For this model there is much better agreement between the model and the data. Figure 22.21 is a similar multiple probability plot using the interaction model. Comparison of the models with and without the interaction term, after deleting the (40 V, 130 °C) condition, indicates some lack of fit for the model without interaction (compare the log likelihoods in Table 22.9). Predictions with the interaction model, however, are very pessimistic and much worse than had been expected by the engineers (though not as easily dismissed as the with the interaction model when fitted to the complete data set). The estimates at use conditions are highly sensitive to the model choice because of the rather large amount of extrapolation involved in computing the estimates. The engineers were uncertain as to the correct model, but felt that almost certainly the truth would lie between the two different fits shown in Figs. 22.20 and 22.21.

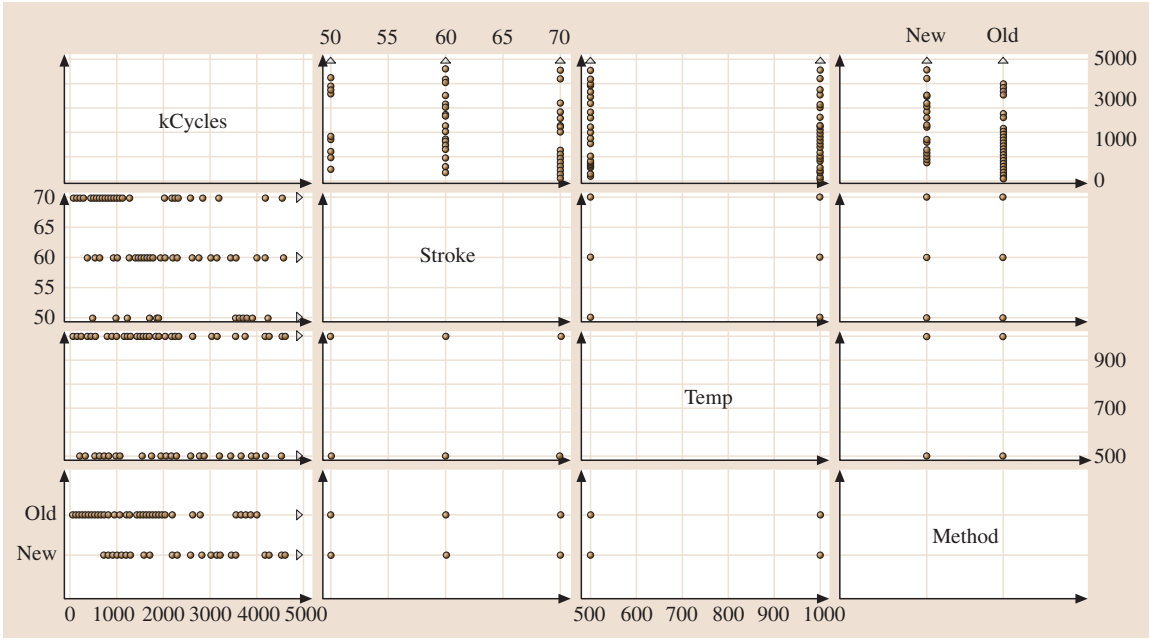

Fig. 22.22 Spring fatigue data. Scatter-plot matrix of the data

Example 22.15: An Accelerated Life Test for a Spring with Three Explanatory Variables. *Meeker*, *Escobar*, and *Zayac* [22.29] describe an experiment to compare old and new processing methods for manufacturing a spring. The experimenters used three variables, namely, stroke displacement (Stroke), processing method (Method), and temperature (temp). Springs were compressed cyclically and Stroke measured the distance that a spring was compressed. Stroke was the accelerating variable. Lifetime was measured in cycles to failure. The springs were designed to be used at Stroke= 20 mils (1 mil =1/1000 inch) and the nominal processing temperature was temp = 600 °F. The goals of the experiment were to compare the old and new processing methods, to see if temperature had an important effect on spring life, and to check if the B10 life (0.10 quantile) at use conditions was at least 500 000 kilocycles.

Meeker, *Escobar*, and *Zayac* [22.29] give the results from a 2×2×3 factorial with factors Stroke (50 mil, 60 mil, 70 mil), temp (500 °F, 1000 °F), and Method (Old, New). Each of the 12 factor combinations was replicated nine times for a total of 108 observations. All nine observations at Stroke= 60, temp = 500 °F, and Method= New were right-censored at 500 000 cycles. Figure 22.22 is a scatter-plot matrix of the Spring ALT data. It appears that on average, spring lifetimes are longer at shorter stroke, at lower temperature, and with the new processing method, respectively.

Figure 22.23 gives Weibull probability plots of the data at individual conditions (factor combinations). The plot indicates that the Weibull distribution can be used to describe the data. Moreover, the plotted lines showing the ML estimates of fraction failing as a function of time at each test condition suggest that it is reasonable to assume that σ (or, equivalently, the Weibull shape parameter β) is constant. The likelihood ratio test for homogeneity of the Weibull shape parameters provides no evidence of differences. Thus, one can assume constant σ across experimental factor combinations.

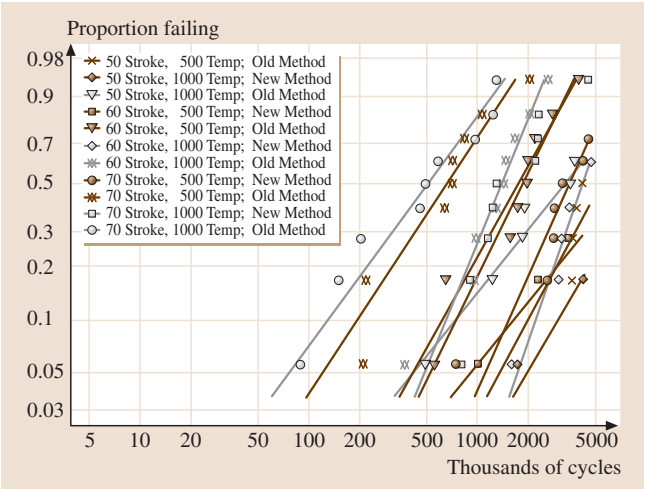

Fig. 22.23 Spring fatigue data. Weibull multiple probability plot with individual Weibull ML fits for each test condition

The model for the location parameter μ was developed as follows. Previous experience with testing similar springs suggested taking a log transformation of Stroke. On the other hand, no transformation is applied to temp because there were no prior studies involving temp (note that because temp is a processing temperature rather than a temperature driving a chemical reaction, there is no suggestion from physical/chemical theory that the Arrhenius relationship should be used). An indicator variable was used to represent the effect of the qualitative factor Method. Thus,

$$\mu = \beta_0 + \beta_1 \log(\text{Stroke}) + \beta_2\, \text{temp} + \beta_3\, \text{Method} \qquad (22.14)$$

where Method = 0 for the New processing method and Method = 1 for the Old method. Terms representing factor interactions can be added to (22.14). *Meeker* et al. [22.29] extended (22.14) to include two-factor interaction terms. The likelihood-ratio test suggested,

Table 22.10 Spring fatigue data. ML estimates for the Weibull regression model

Parameter	ML estimate	Standard error	Normal-approximation 95% confidence interval
β_0	32.03	2.48	[27.16, 36.90]
β_1	−5.51	0.59	[−6.66, −4.36]
β_2	−0.000 88	0.000 27	[−0.0014, −0.000 35]
β_3	−1.27	0.15	[−1.56, −0.98]
σ	0.57	0.054	[0.47, 0.69]

The maximum total log likelihood for this model is $\mathcal{L}_{10} = -625.8$

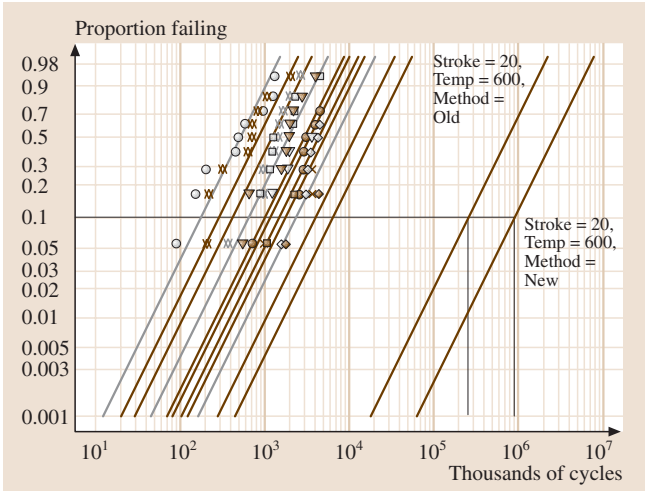

Fig. 22.24 Spring fatigue data. Weibull multiple probability plot of the Weibull regression ML fit with estimates at use conditions

however, that there was little evidence for such interactions.

Table 22.10 gives the results of fitting the Weibull model with the location parameter given in (22.14) and constant σ. For this fit, Fig. 22.24 is a probability plot showing the ML estimates for fraction failing as a function of time for each of the 12 factor combinations and for the Old and New processing methods at use conditions of Stroke = 20 mils and temp = 600 °F. We note the following:

- The estimate and confidence interval for β_1, the coefficient for Stroke, are negative, which suggests that, with temp and Method held constant, increasing Stroke shortens spring life, on average. A similar analysis shows that increasing temperature decreases the life of the units.
- The estimate for the coefficient β_3 for Method is $\hat{\beta}_3 = -1.27 < 0$ and the corresponding confidence interval excludes 0. Thus, there is evidence that switching from the Old to the New method lengthens spring life, on average. In Fig. 22.24, observe that the fraction-failing estimate for the New method is to the right (suggesting longer lives) of the fraction failing for the New method. On the average, springs under the New method last $1/\exp(\hat{\beta}_3) = 3.56$ times longer than those under the Old method. A 95% confidence interval for this factor is [2.66, 4.76] which is obtained by taking the reciprocal of the antilog of the endpoints of the confidence interval for β_3 in Table 22.10.

For a graphical comparison of quantile estimates under the two processing methods, draw horizontal lines in Fig. 22.24 that intersect the New and Old fraction-failing lines, and read off the estimates from the horizontal time axis. Estimates of the 0.10, 0.50 and 0.90 quantiles for the two processing methods under use conditions are given in Table 22.11. This table also provides estimates of the standard errors of quantile estimators and 95% normal-approximation confidence intervals. Observe that quantile estimates for the New method are 3.57 times larger than those for the Old method.

The design engineers wanted to know if the B10 life at use conditions would exceed 500 000 kilocycles. Line segments are drawn in Fig. 22.24 to indicate the B10 estimates. The Old method fails to satisfy this requirement because its B10 life estimate is 252 208 kilocycles. The estimate for the New method is 900 222 kilocycles, which does satisfy the requirement. The lower endpoint of the confidence interval is, however, below the 500 000 target. Thus, there is some doubt that the New method meets the reliability requirement.

Example 22.16: Sensitivity Analysis for the Spring Fatigue Data. Meeker et al. [22.29] studied the effect that varying model assumptions has on the analysis of the spring fatigue data. In particular, they investigated the sensitivity of the estimate of B10 life to alternative transformations of Stroke and temp, and the assumed distribution. A summary of their findings follows.

Table 22.11 Spring fatigue data. Quantiles ML estimates at (20 mil, 600 °F) for the Old and New processing methods

Processing method	Quantile	ML estimate	Standard error	Normal-approximation 95% confidence interval
Old	0.10	252 208	160 148	[72 654, 875 502]
	0.50	737 371	483 794	[203 801, 2 667 873]
	0.90	1 460 875	989 321	[387 409, 5 508 788]
New	0.10	900 221	612 067	[237 471, 3 412 619]
	0.50	2 631 947	1 855 063	[661 194, 10 476 722]
	0.90	5 214 400	3 794 441	[1 252 557, 21 707 557]

Meeker et al. [22.29] extended (22.14) to

$$\mu = \beta_0 + \beta_1 \mathrm{W} + \beta_2 \mathrm{temp} + \beta_3 \mathrm{Method}\,, \qquad (22.15)$$

where

$$\mathrm{W} = \begin{cases} \dfrac{(\mathrm{Stroke})^{\lambda} - 1}{\lambda}, & \lambda \neq 0 \\ \log(\mathrm{Stroke}), & \lambda = 0 \end{cases} \qquad (22.16)$$

and where λ was allowed to range between -1 and 2. The transformation W is known as a Box–Cox transformation, and the linear (no transformation, $\lambda = 1$) and log ($\lambda = 0$) relationships are special cases of this transformation. *Meeker* et al. [22.29] used a range of fixed values of λ and fitted by ML methods a Weibull distribution with μ in (22.15) and constant σ. They observed that, as λ moved from -1 to 2, the ML estimate of the B10 life at use conditions decreased by a factor of between 10^3 and 10^4. In particular, switching from $\lambda = 0$ to $\lambda = 1$ decreased the B10 life estimate from 900 221 kilocycles to 84 925 kilocycles. From past experience with the spring, the engineers thought that λ should be close to 0 and almost certainly less than 1. Thus, a conservative approach for designing the product using the spring as a component would be to assume that $\lambda = 1$.

Using a similar sensitivity analysis with temperature, *Meeker* et al. [22.29] observed that the estimate of B10 life was not as sensitive to temp as it was to Stroke. Increasing λ from -1 to 2 increased the B10 life estimate by no more than a factor of 1.25. They also explain that the data did not provide any information about what transformation (λ value) would be best for model fitting (because there were only two levels of temperature in the experiment).

Another sensitivity analysis involved fitting a lognormal (instead of Weibull) distribution with a location parameter given by (22.15) and constant σ. For any fixed value of λ between -1 and 2, the lognormal distribution gave more optimistic estimates of B10 life than the Weibull distribution. In particular, the lognormal estimates of B10 life were about twice as large as the Weibull estimates. This is expected because, when both distributions are fitted to the same data, the Weibull distribution is less optimistic when extrapolating in time.

22.6 Practical Considerations for Interpreting the Analysis of ALT Data

Extrapolation is an integral part of any ALT. As a result, interpretation of statistical analysis of ALT data is often a challenge. In this section, we discuss the most important issues and suggest strategies to address them.

ALTs are most effective when predicting the life for well-understood failure mechanisms for relatively simple materials or components. ALTs are less useful or there may be more restrictions for more complicated products. There are also difficulties when there are discrepancies between laboratory and field conditions. In particular, when the ALT model generates failure modes that are different from those seen in the field, the information obtained from an ALT may be difficult or impossible to interpret.

ALTs have a better chance to produce useful results if they are carefully planned with attention to obtaining information about possible failure modes from which the product or material might fail.

- Information from earlier experiences with product prototypes or similar products is important. For example, pilot studies can provide information on which environmental factors and failure modes are relevant relative to customer or field use.
- Knowledge of the physical or chemical nature of product degradation and failure is crucial in providing a basis for the statistical model to be fitted to ALT data. This could provide information on how much extrapolation is justified.
- An obvious way to limit the effect of extrapolation is to test at lower levels of the accelerating variables. Doing this, however, results in fewer observed failures, which translates into statistical estimates with larger amounts of uncertainty. For one-variable ALTs, *Meeker* and *Hahn* [22.10] provided practical guidelines for choosing ALT plans that meet practical constraints and have good statistical efficiency.

22.7 Other Kinds of ATs

Discussions up to this point pertain to ALTs where products are tested at high levels of the accelerating variables and extrapolating to assess life at use levels of these variables. Of primary interest is the life distribution with

respect to a few simple failure mechanisms. This section briefly discusses other types of ATs that are used in assessing or improving product reliability. See *Meeker* and *Escobar* ([22.3], Chapt. 19) and references therein for more detailed discussion of these tests and other references.

22.7.1 Continuous Product Operation Accelerated Tests

In this type of AT, tests are performed on the complete system. Such tests are useful because, in addition to testing individual components, the tests can catch problems with component interfaces that cannot be tested in low-level ALTs. In these tests, a sample of product is tested on a more or less continuous basis to accelerate failure mechanisms. Applications include accelerated testing of engines (e.g., in automobiles, motorcycles, lawn equipment, washing machines) and refrigerator compressors. Caution is taken to avoid damage to the system that would not occur in actual product use (e.g., overheating or melted parts due to extreme temperatures). In automobile engine testing, there is one test standard in which the engine is run continuously and another in which the engine is cycled on and off continuously. This is because the two different ATs will tend to generate different kinds of failures.

22.7.2 Highly Accelerated Life Tests

In highly accelerated life tests HALT, products are operated under extremely high levels of variables such as temperature (−90 °C to 190 °C), vibration (up to 60 Grms), and other stresses directly related to system operation. These tests are used to identify failure modes and determine product operational limits. It is generally agreed that these tests provide little or no information about product life at use conditions. This is because the results of the tests usually lead to product design changes. HALTs are typically performed on solid-state electronics, but, with proper equipment, they can be applied to other products as well. *Confer* et al. [22.30] remarked that HALTs can be used to inspect lots of incoming components and to screen products by burn-in. At extremely high levels of the stressing variables, the failure-mechanism model may no longer hold or the system experiences some damage. Thus, precautions must be taken to avoid these effects. See, for example, *McLean* [22.31] and *Hobbs* [22.32] for more information on HALT methods.

22.7.3 Environmental Stress Tests

These tests are closely related to HALTs in that the main objective is to identify reliability issues quickly (e.g., product design flaws) and address them while in the product-development stage. Different authors have different names for this type of test. One is stress–life (STRIFE) tests in which one or two prototypes are aggressively tested to produce failures quickly. Most common STRIFE tests involve temperature and vibration that are cycled in increasing amplitudes throughout the test. *Nelson* ([22.1], pages 37–39) refers to such tests as 'elephant tests.' He described tests of ceramic cookware exposed to cycles of high and low temperature until failure. Failures occurring in these tests are often due to design flaws in the product. Thus, this type of test allows engineers to identify design flaws and fix them while in the design stage. Also, the engineers must determine if failures due to these flaws would occur in actual to avoid unnecessary product redesign. *Nelson* ([22.1], pages 38–39) describes an example where a transformer was redesigned to eliminate a failure mode that was discovered in an elephant test. Years later it was realized that none of the transformers with the old design ever failed from this failure mode; the expensive redesign had been unnecessary.

Nelson ([22.1], Chapt. 1) and *Meeker* and *Escobar* ([22.3], pages 519–520) give more detailed discussions of issues related to environmental stress tests.

22.7.4 Burn-In

Early failures (infant mortality) are the most common problem with electronic products. Defective components, sometimes called freaks, comprise a small fraction of all products and are caused by manufacturing defects. Burn-in involves operating the units at higher that usual levels of accelerating variables for a specific length of time to screen out such defects. For example, burn-in of products such as integrated circuits involve testing units at high levels of temperature and humidity. Units that survive this burn-in period are then put into service. This type of test is expensive because it is essentially a 100% inspection of products. Also, the longer the burn-in period, the more defective items are identified. Tradeoffs between these and other considerations are studied to determine the length of the burn-in period. *Jensen* and *Petersen* [22.33] describe some of the engineering issues related to burn-in. *Kuo* et al. [22.34] discuss statistical and economic issues of burn-in.

22.7.5 Environmental Stress Screening

Environmental stress screening (ESS) methods were developed to improve traditional burn-in tests. It has been suggested that ESS is less expensive and more effective in detecting defectives from the product population. In ESS, products are tested at milder, but more complex, stress processes than in burn-in tests. The methodology has been developed mostly along engineering considerations. The goal is still to screen out defectives without causing damage to the systems. It is widely used in consumer, industrial, and military electronics manufacturing. *Nelson* ([22.1], pages 39–40) provided references regarding ESS military standards and more in-depth discussions of ESS.

22.8 Some Pitfalls of Accelerated Testing

This section reviews potential difficulties one may face in the analysis and interpretation of ALT data. See *Meeker* and *Escobar* [22.35] for a more detailed discussion of these pitfalls.

22.8.1 Failure Behavior Changes at High Levels of Accelerating Variables

It is possible that failure mechanisms at high levels of the accelerating variables may not be the same as those at low levels. High levels of the accelerating variables could induce failure modes that have not been identified beforehand or which may not occur in normal use of the product. Such failure modes can be direct results of physical changes brought on by extreme stressing (e.g., at high temperatures product parts could warp or melt). Also, even with the same failure mechanism, the assumed relationship between life and the accelerating variable(s) may not be valid at higher levels. For example, in a voltage-accelerated ALT, the relationship between log(Life) and log(volt) may not be linear at higher levels of volt.

Previously unrecognized failure modes could still be accounted for in the data analysis by regarding failures caused by them as right-censored with respect to the failure mode of primary interest. This approach, however, requires the assumption of independent failure modes. *Nelson* ([22.1], Chapt. 7) discusses methods for analyzing failure data with competing failure modes, but the failure modes at the higher levels of the accelerating variables restrict the amount of information that will be available on the mode of interest. If possible, the investigator should establish limits on the accelerating variables within which only the primary failure mode occurs and the assumed ALT model holds.

In some applications there will be an effort to eliminate a particular failure mode that is seen only at higher levels of stress. This would be done to make it possible to study another failure mode of primary interest more effectively.

22.8.2 Assessing Estimation Variability

Estimates from ALTs will contain statistical uncertainty due to having only a limited amount of data. It is unsafe to base product-design decisions on point estimates alone. Instead, conclusions from data analysis should account for statistical uncertainty by using confidence intervals. Such confidence intervals provide a range of plausible values for quantities of interest. All of our examples have presented such confidence intervals. Recall the analysis of the GAB insulation data in Example 22.2. Estimates and corresponding pointwise 95% confidence intervals for the fraction failing at $\text{volt}_U = 120$ are shown in Fig. 22.7. The confidence interval for the probability of failure before 5×10^5 h is [0.0017, 0.94]. This interval is too wide to be of any practical value. There are ways to reduce statistical uncertainty (reduce confidence interval width). In general, one could, for instance, increase the sample size, observe more failures by testing at higher stress levels, or reduce the amount of extrapolation. One could also use prior information to fix the values of model parameters that would normally be estimated from data, if there is good information about such parameters. Recall the analyses of the IC device data in Examples 22.10 and 22.11. In the first analysis, all model parameters, including the activation energy E_a, were estimated and pointwise confidence intervals for the fraction failing at use condition temp $= 100\,^\circ\text{C}$ are given in Fig. 22.12. Figure 22.14 is a similar plot for the second analysis with E_a fixed at 0.8 eV, resulting in much narrower confidence intervals. Of course, conclusions from an analysis like that shown in Fig. 22.14 could be misleading if E_a were to be misspecified. *Meeker* and *Escobar* ([22.3], Sect. 22.2) discuss applications of Bayesian analysis

where prior distributions are set up to reflect information about model parameters.

It is important to recognize that the uncertainty reflected in confidence intervals does not include the error (bias) that results from fitting an incorrect model (and strictly speaking, no statistical model is exactly correct). More extrapolation will exacerbate the problem. So, it is important to do sensitivity analysis to study the effect that changes in the model assumptions will have on the results. For example, one could study how estimates and confidence intervals change when the form of the stress-life relationship and/or distribution is changed, as was done in several of the examples in this chapter.

22.8.3 Degradation and Failure Measured in Different Time Scales

In certain applications, lifetime is measured in different time scales (e.g., cycles or hours to failure) depending on which factors affect the degradation process. Often, time scales are determined by how the product is actually used. Incandescent light bulb burn time drives a filament-evaporation process, leading to eventual failure. One way to speed up time is by increasing voltage. The bulb is operated continuously and lifetime is measured in hours of operation. Also, turning a light bulb on and off produces mechanical shocks that can cause the initiation and growth of fatigue cracks within the filament. Bulb life in this case might be measured in on–off cycles. Testing bulbs continuously at higher voltages does not simulate the on–off cycling effect. Thus, predictions based on a simple model with only one time scale will not accurately describe light bulbs that fail through a combination of burn time and on–off cycles.

22.8.4 Masked Failure Modes

In some situations, higher levels of the accelerating variable can produce a new failure mode, not ordinarily seen at use conditions. This new failure mode can mask the failure mode of interest. If the new failure mode is not recognized (because engineers naively think they are the same and do not check), the resulting conclusions will be highly optimistic relative to the truth. See *Meeker* and *Escobar* ([22.3], Fig. 19.22) for an illustration and further discussion.

22.8.5 Differences Between Product and Environmental Conditions in Laboratory and Field Conditions

For accurate prediction of failure behavior in the field, it is necessary that laboratory conditions be similar to those in the field, and that units tested in the laboratory be similar to products in actual use. Laboratory conditions are not always similar to field conditions. For example, in a life test of a circuit pack, accelerated levels of temperature resulted in lower humidity levels. This in turn inhibited corrosion, which was the primary cause of failure in the field. Thus, there were more failures in the field than were predicted by the data analysis. Laboratory tests should have controlled both temperature and humidity levels. Also, laboratory tests are generally carefully controlled, while in actual use, the environment may be highly variable.

There are various points in the process from prototype development to product manufacture at which product-building inconsistencies could occur. Technicians may build prototypes to be used in testing in a manner that is different from the way an assembly line builds the final product. For example, products with epoxy have to be cured for a certain length of time in an oven. Uncured epoxy can be highly reactive and may cause corrosion and lead to premature failure. It is possible that the units are effectively cured in the lab, but not in the factory assembly line. ALT tests will likely predict failure behavior that is more optimistic than that in the field. Raw materials and instruments could also vary. It is also possible, because of identified design flaws, to modify the product design several times throughout the process. Any inconsistencies in how a product is built will most likely cause disagreements between laboratory and field results.

22.9 Computer Software for Analyzing ALT Data

Nelson ([22.1], pages 237–240) provides a table listing software packages for analysis of ALT data by maximum likelihood methods (which has been updated in the 2004 paperback edition). The table provides the packages' features and specific capabilities. Commercially available statistical software such as SAS JMP [22.36], SAS [22.37], MINITAB [22.38], and S-PLUS [22.39] have procedures specifically for ALT data analysis.

ALTA [22.40] is a software package specifically for ALT analysis.

All of the analyses in this chapter were done with S-PLUS Life Data Analysis (SPLIDA) by *Meeker* and *Escobar* [22.41]. SPLIDA runs on top of S-PLUS. Special features for some plots were created by modifying SPLIDA functions and using S-PLUS annotation tools. SPLIDA consists of special S-PLUS functions and GUIs, and is available for download from http://www.public.iastate.edu/~splida/. The SPLIDA download also contains files with all of the data sets from this chapter, as well as many other example data sets, including all examples from *Meeker* and *Escobar* [22.3] and many from *Nelson* [22.1].

References

22.1 W. Nelson: *Accelerated Testing: Statistical Models, Test Plans, Data Analyses* (Wiley, New York 1990)

22.2 P. A. Tobias, D. C. Trindade: *Applied Reliability*, 2nd edn. (Nostrand Reinhold, New York 1995)

22.3 W. Q. Meeker, L. A. Escobar: *Statistical Methods for Reliability Data* (Wiley, New York 1998)

22.4 W. Q. Meeker, M. Hamada: Statistical tools for the rapid development & evaluation of high-reliability products, IEEE Trans. Reliab. **44**, 187–198 (1995)

22.5 W. Q. Meeker, L. A. Escobar: Reliability: the other dimension of quality, Qual. Technol. Qual. Man. **1**, 1–25 (2004)

22.6 L. A. Escobar, W. Q. Meeker, D. L. Kugler, L. L. Kramer: Accelerated destructive degradation tests: data, models, and analysis. In: *Mathematical, Statistical Methods in Reliability*, ed. by B. H. Lindqvist, K. A. Doksum (World Scientific, Singapore 2003)

22.7 D. R. Johnston, J. T. LaForte, P. E. Podhorez, H. N. Galpern: Frequency acceleration of voltage endurance, IEEE Trans. Electr. Insul. **14**, 121–126 (1979)

22.8 N. E .Dowling: *Mechanical Behavior of Materials* (Prentice Hall, Englewood Cliffs 1993)

22.9 D. J. Klinger: Failure time and rate constant degradation: an argument for the inverse relationship, Microelectron. Reliab. **32**, 987–994 (1992)

22.10 W. Q. Meeker, G. J. Hahn: *How to Plan an Accelerated Life Test: Some Practical Guidelines*, ASQC Basic References in Quality Control: Statistical Techniques, Vol. 10 (Am. Soc. Qual. Control, Milwaukee

22.11 M. J. LuValle, T. L. Welsher, K. Svoboda: Acceleration transforms and statistical kinetic models, J. Stat. Phys. **52**, 311–320 (1988)

22.12 N. Doganaksoy, G. J. Hahn, W. Q. Meeker: Accelerated testing for speedier reliability analysis, Qual. Prog. **36**, 58–63 (2003)

22.13 K. C. Boyko, D. L. Gerlach: Time dependent dielectric breakdown of of 210 oxides, Proc. IEEE Int. Reliab. Phys. Symp. **27**, 1–8 (1989)

22.14 J. Klinger D. On the notion of activation energy in reliability: Arrhenius, Eyring, and thermodynamics, Proceedings of the Annual Reliability, Maintainability Symposium (IEEE, New York 1991) 295–300

22.15 F. M. d'Heurle, P. S. Ho: Electromigration in thin films. In: *Thin Films–Interdiffusion and Reactions*, ed. by J. M. Poate, K. N. Tu, J. W. Mayer (Wiley, New York 1978) pp. 243–303

22.16 P. B. Ghate: Electromigration–induced failures in VLSI interconnects, Proc. Int. Reliab. Phys. Symp. **20**, 292–299 (1982)

22.17 J. R. Black: Electromigration–a brief survey and some recent results, IEEE Trans. Electron. Dev. **16**, 338–347 (1969)

22.18 K. T. Gillen, K. E. Mead: *Predicting life expectancy and simulating age of complex equipment using accelerated aging techniques, National Technical Information Service* (U.S. Department of Commerce, Springfield 1980)

22.19 D. J. Klinger: Humidity acceleration factor for plastic packaged electronic devices, Qual. Reliab. Eng. Int. **7**, 365–370 (1991)

22.20 M. J. LuValle, T. L. Welsher, J. P. Mitchell: A new approach to the extrapolation of accelerated life test data, The Proc. of the Fifth Int. Conf. Reliability and Maintainability (Tech. Dig., Biarritz 1986) 620–635

22.21 G. Boccaletti, F. D'Esponosa, F. R. Borri, E. Ghio: Accelerated tests. In: *Microelectronic Reliability, Volume HI, Reliability, Integrity Assessment and Assurance*, ed. by E. Pollino (Artech House, Norwood 1989) Chapt. 11

22.22 W. B. Joyce, K-Y Liou, F. R. Nash, P. R. Bossard, R. L. Hartman: Methodology of accelerated aging, AT&T Tech. J. **64**, 717–764 (1995)

22.23 D. S. Peck: Comprehensive model for humidity testing correlation, Proc. Int. Reliab. Phys. Symp. **24**, 44–50 (1986)

22.24 D. S. Peck, C. H. Or. Zierdt: The reliability of semiconductor devices in the Bell system, Proc. IEEE **62**, 185–211 (1974)

22.25 H. Eyring, S. Gladstones, K. J. Laidler: *The Theory of Rate Processes* (McGraw Hill, New York 1941)

22.26 H. Eyring: *Basic Chemical Kinetics* (Wiley, New York 1980)

22.27 MIL-STD-883: *Test Methods and Procedures for Microelectronics* (Naval Publ. Forms Center, Philadelphia 1985)

22.28 T. Shimokawa, Y. Hamaguchi: Statistical evaluation of fatigue life and fatigue strength in

circular-holed notched specimens of a carbon eight-harness-satin/epoxy laminate. In: *Statistical Research on Fatigue and Fracture*, Cur. Mater. Res., Vol. 2, ed. by T. Tanaka, S. Nishijima, M. Ichikawa (Elsevier Applied Science, London 1987) pp. 159–176

22.29 W. Q. Meeker, L. A. Escobar, S. A. Zayac: Use of sensitivity analysis to assess the effect of model uncertainty in analyzing accelerated life test data. In: *Case Studies in Reliability and Maintenance*, ed. by W. R. Blischke, D. N. P. Murthy (Wiley, New York 2003) Chapt. 6

22.30 R. Confer, J. Canner, T. Trostle: Use of highly accelerated life test (HALT) to determine reliability of multilayer ceramic capacitors, Proc. Electron. Comp. Technol. Conf. **41**, 320–322 (1991)

22.31 H. McLean: *HALT, HASS and HASA Explained: Accelerated Reliability Techniques* (ASQ Quality, Milwaukee 2000)

22.32 G. K. Hobbs: *Accelerated Reliability Engineering: HALT and HASS* (Wiley, New York 2000)

22.33 F. Jensen, N. E. Petersen: *Burn-In: An Engineering Approach to Design, Analysis of Burn-In Procedures* (Wiley, New York 1982)

22.34 W. Kuo, W. T. K. Chien, T. Kim: *Reliability and Stress Burn-In* (Kluwer Academic, Dordrecht 1998)

22.35 W. Q. Meeker, L. A. Escobar: Pitfalls of accelerated testing, IEEE Trans. Reliab. **47**, 114–118 (1998)

22.36 SAS Institute Inc.: JMP User's Guide, Version 5.1.1 (SAS Institute, Cary 2004) http://www.jmp.com/

22.37 SAS Institute Inc.: *SAS/QC® Software: Changes and Enhancements, Release 8.2* (SAS Institute, Cary 2001) http://www.sas.com/statistics/

22.38 MINITAB: *MINITAB User's Guide 2: Data Analysis, Quality Tools* (Minitab, Inc. State College 2000) http://www.minitab.com/

22.39 SPLUS 6.2: *Guide to Statistics*, Vol. 2 (Insightful Corp., Seattle 2001) http://www.insightful.com/

22.40 ALTA: *ALTA Version 6 User's Guide* (Reliasoft, Tucson 2002)

22.41 W. Q. Meeker, L. A. Escobar, SPLIDA User's Manual (Iowa State Univ., Ames 2004) Available at http://www.public.iastate.edu/~splida